This is a preprint, the final version is subject to change, of the American Mineralogist (MSA)
Cite as Authors (Year) Title. American Mineralogist, in press.
DOI: https://doi.org/10.2138/am-2020-6972

Revision 2

Hornblende as a Tool for Assessing Mineral-Melt Equilibrium and Recognition of Crystal Accumulation

Kevin Werts[1], Calvin G. Barnes[1], Valbone Memeti[2], Barbara Ratschbacher[3] Dustin Williams[2], Scott Paterson[4]

[1]Department of Geosciences, Texas Tech University, Lubbock, Texas 79409-1053, U.S.A.

[2]Department of Geological Sciences, California State University, Fullerton, California 92834-6850, U.S.A.

[3]Division of Geological and Planetary Sciences, California Institute of Technology, Pasadena, California 91125, U.S.A.

[4]Department of Earth Sciences, University of Southern California, Los Angeles, California 90089, U.S.A.

ABSTRACT

Bulk-rock compositions are commonly used as proxies for melt compositions, particularly in silicic plutonic systems. However, crystal accumulation and/or melt loss may play an important role in bulk-rock compositional variability (McCarthy and Hasty, 1976; McCarthy and Groves, 1979; Wiebe, 1993; Wiebe et al., 2002; Collins et al., 2006; Deering and Bachmann, 2010; Miller et al., 2011; Vernon and Collins, 2011; Lee and Morton, 2015; Lee et al., 2015; Barnes et al., 2016a; Schaen et al., 2018). Recognizing and quantifying the effects of crystal

accumulation and melt loss in these silicic systems is challenging. Hornblende-melt Fe/Mg partitioning relationships and hornblende (Hbl) chemometry are used here to test for equilibrium with encompassing bulk-rock and/or glass compositions from a number of plutonic and volcanic systems. Further, we assess the extent to which these tests can be appropriately applied to Hbl from plutonic systems by investigating whether Hbl from the long-lived (~ 10 m.y.) Tuolumne Intrusive Complex preserves magmatic crystallization histories. On the basis of regular zoning patterns, co-variation of both fast- and slow-diffusing trace elements, Hbl thermometry, and compositional overlap with volcanic Hbl we conclude that Hbl from plutons largely preserve records supporting the preservation of a magmatic crystallization history, although many compositional analyses yield calculated temperatures < 750°C, which is unusual in volcanic Hbl.

Hornblende is only rarely in equilibrium with host plutonic bulk-rock compositions over a wide-range of SiO_2 contents (42–78 wt%). Hornblende chemometry indicates that the majority of Hbl from the plutonic systems investigated here is in equilibrium with melts that are typically more silicic (dacitic to rhyolitic in composition) than bulk-rock compositions. These results are consistent with crystal accumulation and/or loss of silicic melts within middle- to upper-crustal plutons. Although the processes by which melts are removed from these plutonic systems is uncertain, it is evident that these melts are either redistributed in the crust (e.g. leucogranite dikes, plutonic roofs, etc.) or are instead erupted. In contrast, Hbl from volcanic rocks is more commonly in equilibrium with bulk-rock and glass compositions. In most cases, where Hbl is out of equilibrium with its host glass, the glasses are more evolved than the calculated melts indicating crystallization from a less fractionated melt and/or mixed crystal populations. Where Hbl is not in equilibrium with volcanic bulk-rocks, the bulk-rock compositions are typically more mafic than the calculated melts. In some intermediate volcanic samples, the occurrence of

wide-ranges of calculated melt compositions is indicative of magma mixing. The general absence of Hbl with temperatures < 750°C from volcanic systems suggests that magmatic mushes below this temperature are unlikely to erupt. Our results indicate that bulk-rock compositions of granitic plutonic rocks only rarely approximate melt compositions and that the possibility of crystal accumulation and/or melt loss cannot be ignored. We suggest that detailed assessments of crystal accumulation and melt loss processes in magmatic systems is crucial to evaluating magma differentiation processes and discerning petrogenetic links between plutonic and volcanic systems.

Keywords: hornblende, crystal accumulation, granite, rhyolite, volcano – plutonic connection

Corresponding Author: kevin.werts@ttu.edu

INTRODUCTION

Bulk-rock compositional trends in quartz-bearing plutonic rocks are commonly used to infer magma evolution. Traditionally, magmatic processes such as fractional crystallization (Bowen, 1928), magma mixing (Reid et al., 1983; Davidson et al., 2001), and assimilation (DePaolo, 1981; Spera and Bohrson, 2001) are the primary magmatic processes considered in the modeling of these bulk-rock compositions. However, the effect of crystal accumulation on compositional trends is less commonly considered (but see McCarthy and Hasty, 1976; McCarthy and Groves, 1979; Wiebe, 1993; Wiebe et al., 2002; Collins et al., 2006; Deering and Bachmann, 2010; Miller et al., 2011; Vernon and Collins, 2011; Lee and Morton, 2015; Lee et al., 2015; Barnes et al., 2016a; Schaen et al., 2018). Thus, the implicit assumption in many petrological studies is that bulk-rock compositions approximate melt compositions and that they

can be used to model other magmatic processes (i.e. fractionation, mixing, assimilation). Crystal accumulation and/or melt loss may be difficult to recognize in evolved magmatic systems given that evidence supporting these processes may be cryptic at the outcrop scale (Weinberg, 2006; Vernon and Collins, 2011) and because compositional trends driven by accumulation may follow a similar yet opposite trajectory to crystal fractionation trends (Deering and Bachmann, 2010). The use of bulk-rock compositions as input for modeling of magmatic processes (e.g. MELTS modeling) or in saturation thermometry (e.g. zircon and apatite saturation) may therefore be problematic, particularly in plutonic systems where any direct evidence of melt compositions such as quenched glasses is absent.

The occurrence and extent of crystal accumulation in plutons has important implications for discerning whether genetic links exist between plutonic and volcanic rocks as well as for identifying the location(s) and the extent of magma differentiation in the crust (Keller et al., 2015). For example, some authors have argued that magma differentiation is mainly restricted to lower crustal hot zones (e.g., Hildreth and Moorbath, 1988; Annen et al., 2006) and that the heterogeneity of plutons is primarily related to the diversity of melts produced from these hot zones (Coleman et al., 2004; 2012). These models suggest that magma addition rates into middle and upper crustal magma bodies is too low to allow for significant amounts of magma differentiation. Other authors argue that magma differentiation processes (e.g. crystal-liquid separation) may be important within middle and upper crustal magma bodies during high magma addition rate events (Bachmann and Bergantz, 2004; 2008; Hildreth, 2004; Bachmann et al., 2007; Lipman, 2007; Paterson et al., 2011; 2016; Lipman and Bachmann, 2015). One approach that has been taken to address this problem is to place mass-balance constraints between eruptive products and their complementary residues; however, this approach requires that melt

compositions are known (Gelman et al., 2014: Lee and Morton, 2015). An alternative approach is to identify a means by which individual bulk-rocks or bulk-rock compositions can be evaluated to determine whether the sample approximates a melt or instead represents a cumulate or some combination of cumulate ± melt. At the outcrop scale, crystal accumulation is typically discerned on the basis of excessive localization of mineral phases (e.g. schlieren, K-feldspar megacryst rich clusters) or from the abundances of cumulus to intercumulus phases. Thin-section scale studies placing textural constraints on crystal accumulation and melt loss are also useful, although the uncertainties surrounding ways to visually recognize the relative importance of individual accumulation and/or melt loss processes may hinder our ability to quantify their extents (Holness, 2018; Schaen et al., 2018).

Independent constraints on crystallization conditions (i.e. melt composition, temperature, pressure, fugacity of volatiles) and magmatic processes can potentially be discerned through mineral compositions and intracrystalline zoning patterns. For example, several recent studies have demonstrated that hornblende (Hbl) compositions can be used to both characterize trace element melt compositions and to track magmatic processes in plutons (Coint et al., 2013a; Barnes et al., 2016a,b,c; 2017; Schaen et al., 2018), while others (Ridolfi and Renzulli, 2012; Putirka, 2016a; Zhang et al., 2017) have proposed that Hbl compositions can be used to estimate equilibrium melt compositions and track apparent changes in temperature. Hornblende compositional variability may therefore be useful for investigating melt differentiation histories and assessing the importance of crystal accumulation and/or melt loss in plutons. However, unlike volcanic systems, where magmas are rapidly quenched, plutons undergo slow cooling with the potential for recrystallization, diffusion, and dissolution-reprecipitation processes to obscure or overprint the original magmatic compositions and/or textural features. It is therefore

117 important to determine the extent to which primary magmatic compositions are preserved in Hbl
118 from plutons. First, we investigate whether Hbl from plutons preserves any record of a magmatic
119 crystallization history or whether wide-spread re-equilibration has occurred during slow cooling.
120 Our study focuses on Hbl from the long-lived (~ 10 Ma) Tuolumne Intrusive Complex (Figure 1)
121 where independent workers have argued both for (Challener and Glazner, 2017) and against
122 (Barnes et al., 2016c) wide-spread re-equilibration of Hbl. We conclude that Hbl from plutons
123 preserves both magmatic and non-magmatic crystallization histories but that evidence of wide-
124 spread re-equilibration is lacking and that petrographic constraints are crucial for discerning
125 primary magmatic zones from those that have undergone re-equilibration at low temperatures.
126 Second, we investigate Hbl–bulk-rock and Hbl–glass equilibrium relationships from a number of
127 plutonic and volcanic systems by employing Hbl–melt $^{Fe/Mg}Kd$ tests (Putirka, 2016a) and Hbl
128 chemometry (Ridolfi and Renzulli, 2012; Putirka, 2016a; Zhang et al., 2017) in order to assess
129 the importance of crystal accumulation and crystal-liquid separation in both plutonic and
130 volcanic systems. This study shows that Hbl from many plutonic and volcanic systems is not in
131 equilibrium with bulk-rock compositions and that in any study of coarse grained-granitic rocks,
132 the effects of crystal accumulation and/or melt loss must be considered in conjunction with other
133 petrogenetic processes.
134

135 **METHODS**

136 Hornblende and bulk-rock major elements from seven plutonic systems (Tuolumne
137 Intrusive Complex, Wooley Creek batholith, and the English Peak, Ashland, Tenpeak, Mt Stuart,
138 and Black Peak plutons) are investigated here along with many Hbl, bulk-rock, and glass
139 analyses from twelve volcanic systems. A summary of each of the data sets used in this study is

presented in Table 1. The plutonic systems are all arc-related mid- to upper-crustal Cordilleran plutonic systems and with the exception of the Fish Canyon magma body, all of the volcanic systems considered here are products of arc magmatism. Bulk-rock compositions are wide-ranging for both the volcanic systems (basalt to rhyolite) and plutonic systems (diorite to granite). The data set includes ~ 7,900 Hbl compositions from the twelve volcanic systems and more than 4,300 compositions from the seven plutonic systems. Some analyses were filtered from the initial data set, including ~ 5% of the Hbl analyses from volcanic systems and < 2% of the Hbl analyses from plutonic systems. These data were removed on the basis of totals (< 95.5 and > 100.5 wt.%), SiO_2 (< 38 and > 59 wt%) and CaO (< 7 and > 15 wt%) content. In addition, any Hbl analyses that were marked as originating from xenoliths, enclaves, veins, or dikes were not considered so as to investigate only those Hbl that constitute the majority of the magmatic system and because it is unclear whether these Hbl share any genetic relationship to the magmatic system. In many cases, individual Hbl analyses are paired with an associated glass and/or bulk-rock composition; thus, tests for Hbl/melt and Hbl/bulk-rock equilibrium can be conducted. Bulk-rock compositional analyses with totals < 97 and > 100.5 wt% were not utilized for these equilibrium tests.

Bulk-rock and Hbl major element compositions are presented here (see Supplementary Data File 1) for several Cordilleran intrusive systems (Tuolumne Intrusive Complex, Wooley Creek batholith, and English Peak, Ashland, Tenpeak, Mt Stuart, and Black Peak plutons). Some mineral compositions were published as "representative data" owing to space limiations. These published data consisted of individual core-rim or core-mantle-rim analyses (Barnes, 1983; Barnes, 1987; Gribble et al., 1990; Coint et al., 2013a), not averaged data. This paper allows publication of the complete data sets. For the Tuolumne Intrusive Complex, a primary

focus of this study, a total of twenty seven samples were analyzed for Hbl compositions (Figure 1). A minimum of three Hbl were analyzed from each sample and at least 5 spots were typically collected from each Hbl. In the earlier work (Barnes, 1983, 1987; Gribble et al., 1990), at least two and generally four to five individual grains were analyzed, with at least three spots per grain.

Hornblende major elements were collected by electron microprobe analysis (EMPA) whereas bulk-rock major element compositions were collected using x-ray fluorescence (XRF) or inductively coupled plasma atomic emission spectrometry (ICP-AES). A description of the methodologies for each set of compositional analyses is presented in Supplementary Data File 2. Bulk-rock, glass, and Hbl compositional data for each of the volcanic systems were collected from the literature (Table 1). For each of the literature-based data sets, major element compositions for Hbl and glasses were acquired by EPMA whereas major element compositions for bulk-rocks were collected by XRF or ICP-OES.

Hornblende structural formulae were calculated on the basis of 23 oxygen atoms using the spreadsheet of Esawi (2004) and classified according to Leake et al. (1997). Apparent crystallization temperatures were calculated using equation 5 from Putirka (2016a), which is a pressure-independent thermometer based on Si, Ti, Na, and Fe, with an uncertainty of ± 30°C.

RESULTS

Textural and Compositional Variability of Hornblende from the Tuolumne Intrusive Complex

Discerning the extent to which Hbl from plutons has experienced compositional modification related to slow cooling and/or subsolidus recrystallization processes (compare

Barnes et al., 2016c to Challener and Glazner, 2017) is critical to its usefulness in assessing mineral-melt equilibrium and evaluating magmatic processes. What follows is a detailed investigation into the relationship between composition and texture/color in Hbl from the Tuolumne Intrusive Complex (TIC).

The TIC is a long-lived (~ 10 Ma) concentrically zoned intrusive complex made up of three major, partially nested rock units: the outer Kuna Crest, the Half Dome, and the innermost unit, the Cathedral Peak (Figure 1) (Bateman and Chappell, 1979). Kuna Crest is the oldest unit and is characterized by abundant anhedral to subhedral Hbl and biotite (Bateman and Chappell, 1979). The Half Dome is instead marked by the occurrence of euhedral Hbl, biotite, and titanite phenocrysts and is separated into both an equigranular outer phase and a porphyritic inner phase (Bateman and Chappell, 1979). Porphyritic Half Dome contains K-feldspar phenocrysts up to ~ 3 cm in length and typically a lower modal abundance of mafic minerals compared to samples from equigranular Half Dome (Bateman and Chappell, 1979). The innermost unit, Cathedral Peak, contains K-feldspar megacrysts that may be > 10 cm in length, cm-sized quartz pools, fewer mafic minerals, and a higher proportion of biotite to Hbl compared to Half Dome and Kuna Crest (Bateman and Chappell, 1979). The contacts between each of the TIC units may vary from knife sharp to gradational over hundreds of meters such that the boundaries between units may be transitional (Bateman and Chappell, 1979; Bateman, 1992; Žák and Paterson 2005; Paterson et al., 2016).

Hornblende from Kuna Crest is typically small (< 1 cm), anhedral to subhedral, and rarely displays petrographic zoning. Some Hbl from Kuna Crest contain cores of pyroxene and/or quartz, indicative of a peritectic reaction of pyroxene to Hbl (Bateman and Chappell, 1979). Hornblende from Half Dome is typically euhedral to subhedral, up to ~ 2 cms in length,

and commonly exhibits patchy zoning. Some Half Dome Hbl is rich in inclusions of other rock forming minerals (e.g. biotite, plagioclase, magnetite, apatite, and less commonly, zircon) (Challener and Glazner, 2017). Hornblende is rare (generally < 2%) in Cathedral Peak, typically small (< 1 cm), subhedral to anhedral, and also displays patchy zoning. Note that patchy color zoning (Figure 2a,b) occurs in Hbl from each of the TIC units but is best displayed in Hbl from Half Dome and Cathedral Peak. Hornblende preserving evidence of concentric zoning is exceedingly rare (Figure 2c) even in Hbl where patchy zoning is generally absent.

The compositions of TIC Hbl range from magnesiohornblende to actinolite (Figure 3) and display little variation from unit to unit. However, Hbl from Kuna Crest is generally characterized by lower Mg# at a given Si (apfu) value compared to Hbl from Half Dome or Cathedral Peak (Figure 3). Hornblende that lacks readily distinguishable petrographic zoning generally displays only small variations in major element compositions (e.g. changes in Si (apfu) < 0.2). These small variations may or may not be systematic from core to rim. Further, these Hbl are typically characterized by calculated crystallization temperatures that are above 750°C, consistent with magmatic crystallization. Alternatively, Hbl exhibiting patchy zoning is typically characterized by a wider-range of compositions (e.g. Si (apfu) variations > 1) and calculated crystallization temperatures (e.g. from 600–800°C).

Many of the complex textural and compositional relationships of TIC Hbl can be illustrated by a cm-sized Hbl from equigranular Half Dome (Figure 2a,b). This Hbl displays patchy zoning and contains inclusions of biotite, plagioclase, magnetite, and apatite. There are at least three texturally distinct zones within the crystal, including an olive-brown to olive-green pleochroic zone which appears to represent the dominant core of the crystal, a pale-green to blue-green pleochroic zone, and a pale olive-colored euhedral rim. The boundaries between the olive-

brown–olive-green and green–blue-green zones are variably sharp to gradational, similar to patchy zoning descriptions given by Challener and Glazner (2017) for other equigranular Half Dome Hbl. The olive-brown–olive-green core zones are magnesiohornblende and are characterized by Si (apfu) < 7.1, Ti (apfu) > 0.09, and crystallization temperatures > 765°C (Figure 4). The pale-green–blue-green zones instead vary from magnesiohornblende to actinolite, with Si (apfu) > 7.3, Ti (apfu) < 0.03, and crystallization temperatures < 715°C (Figure 4). The pale olive-colored rim has Si, Ti, and crystallization temperatures that are intermediate between the olive-brown–olive-green and green–blue-green pleochroic zones (Figure 4). On the basis of temperature calculations, the olive colored zones preserve records of a magmatic crystallization history, whereas pale-green–blue-green zones and the pale olive colored rim potentially represent growth from melt in a static mush or at sub-solidus conditions. Below we compare the compositional trends of Hbl from several plutonic and volcanic suites to further test these conclusions.

Volcanic vs Plutonic Hornblende

The Hbl investigated here originate from a wide compositional range of volcanic (basaltic to rhyolitic) and plutonic (dioritic to granitic) bulk-rocks. However, the glass compositions reported from the volcanic rocks are, with rare exceptions, rhyolitic in composition. The distribution of Hbl compositions from volcanic rocks is 71% magnesiohornblende, 17% tschermakite, 9% magnesiohastingsite, and < 3% edenite/pargasite, whereas 89% of the Hbl from plutonic rocks is classified as magnesiohornblende, 7% as tschermakite, 3% as actinolite, and < 1% edenite/pargasite (Table 1). In general, there is significant compositional overlap between Hbl from the plutonic and volcanic systems, particularly in the Si range of 6.1 to 7.4

(apfu) (Figure 5). Over this range of Si, Hbl from volcanic and plutonic rocks typically produce similar sets of parallel trends (Figure 5, Supplementary Figure 1). However, for some elements such as Al and Na, there are small offsets at a given Si value (Figure 5). For example, Hbl from volcanic systems is generally characterized by lower Al and higher Na at a given Si value compared to Hbl from plutonic systems (Figure 5, Supplementary Figure 1). These differences in Al and Na are also correlated with temperature (Supplementary Figure 2). At a given temperature value, Hbl from the volcanic systems is typically lower in Al and higher in Na compared to Hbl from the plutonic systems (Supplementary Figure 2).

The Hbl from volcanic systems extends to more primitive compositions (i.e. lower Si and higher Ti, Al) and yields higher maximum temperatures of crystallization (T_{max}= 1031°C) compared to Hbl from plutonic systems (T_{max} = 975°C) (Figure 5). Hornblende from plutonic systems instead extends to more evolved compositions (i.e. higher Si, lower Ti, Al) and lower minimum temperatures (T_{min} = 532°C) than Hbl from volcanic systems (T_{min} = 686°C) (Figure 5). Over 95% of the Hbl temperature estimates from volcanic systems yield values above 750°C, with only four analyses (<<1%) below 700°C, whereas 35% of Hbl temperature estimates from plutonic systems yield temperatures below 750°C. Thus, some Hbl analyses from plutons record lower temperature histories that are not typically observed in volcanic systems. Both plutonic and volcanic Hbl are characterized by a large number of calculated temperatures at ~ 760–780°C (Figure 6). However, whereas Hbl from plutons is characterized by a roughly normal distribution, a second temperature peak occurs in Hbl from volcanic systems at ~ 950°C (Figure 6). This high temperature peak primarily results from temperature estimates derived from intermediate and mafic systems such as Redoubt, Yanacocha, Augustine, and Young Shiveluch, although some of the more silicic systems such as Cardones and Mt. St. Helens also display

peaks at high temperatures (see Supplementary Figure 3). Many of the volcanic systems with high temperature Hbl also display bimodal distributions in their calculated temperatures (e.g. Cardones, Redoubt, Yanacocha, Augustine).

In summary, the compositional trends of Hbl from volcanic and plutonic systems displays significant overlap from 6.1 to 7.4 Si (apfu) with small offsets in elements such as Na and Al. However, Hbl from volcanic systems is distinct in that it records higher maximum temperatures and more primitive (i.e. lower Si, higher Ti) compositions compared to Hbl from the plutons investigated in this study. Furthermore, the compositions of Hbl from plutonic systems extend to more evolved values (higher Si, lower Ti) and lower minimum temperatures compared to those from volcanic systems.

Hornblende – Melt Fe/Mg Equilibrium in Plutonic and Volcanic Systems

Studies of mafic magmatic systems commonly utilize mineral-melt Fe/Mg exchange as a test of compositional equilibrium between crystals and melt (or bulk-rock / glass) (e.g. Roeder and Emslie, 1970; Putirka, 2008; 2016b); however, these tests are rarely applied to silicic systems. This is in part because the minerals most commonly utilized to investigate Fe/Mg equilibrium, olivine, augite, and orthopyroxene, typically only occur in hotter and/or drier silicic systems (e.g. Bachmann and Bergantz, 2008; Christiansen and McCurry, 2008). In evolved calc-alkaline systems, biotite and Hbl are the typical ferromagnesian silicates. Recent investigations into Hbl-melt Fe/Mg equilibrium (Putirka, 2016a) and Hbl chemometry (Ridolfi and Renzulli, 2012; Putirka, 2016a; Zhang et al., 2017) provide an important means by which Hbl–bulk-rock and Hbl–glass equilibrium can be evaluated in silicic systems.

The Fe-Mg exchange coefficient or Hbl-melt $^{Fe/Mg}Kd$, is independent of pressure, temperature, and melt composition (Putirka, 2016a). We follow the methods of Putirka (2016a) in calculating the Hbl-melt $^{Fe/Mg}Kd$ as $^{Hbl}Fe^{T}/^{Hbl}Mg$ / $^{Melt}Fe^{T}/^{Melt}Mg$ where ^{Hbl}Fe and ^{Hbl}Mg are cations in Hbl calculated on the basis of 23 oxygen atoms and $^{Melt}Fe^{T}$ and ^{Melt}Mg are Fe^{T} and Mg calculated from the bulk-rock or glass in atomic units. The more conservative estimate for Hbl-melt $^{Fe/Mg}$ Kd equilibrium proposed by Putirka (2016a) is used here in which any Hbl – melt $^{Fe/Mg}$ Kd values that lie between 0.13 and 0.41 are considered to be in equilibrium. For the purpose of studying equilibrium between Hbl and bulk-rock/glass compositions, we restrict our data set to Hbl with Si < 7.0 (apfu) and temperatures > 750°C. These filters are introduced because the chemometric equations from Zhang et al. (2017) (discussed below) are calibrated for 5.7 < Si (apfu) < 7.0, and because we wish to compare Hbl from plutonic systems to compositionally similar Hbl in volcanic systems.

Hornblende-bulk-rock $^{Fe/Mg}$ Kd values for the six plutons range from 0.2 to 2.8 (Figure 7). Only 2% of the > 3000 Hbl-bulk-rock $^{Fe/Mg}$ Kd values from these plutons are in equilibrium. The Hbl-bulk-rock $^{Fe/Mg}$ Kd values for volcanic systems range from 0.1 to 1.5, similar to the range observed from plutonic systems (Figure 7). However, 67% of the ~ 3800 Hbl-bulk-rock $^{Fe/Mg}Kd$ values for volcanic systems indicate Fe/Mg equilibrium. At bulk-rock SiO_2 > 65 wt%, more than 86% of the Hbl compositions from volcanic systems are in Fe/Mg equilibrium, whereas at SiO_2 < 65 wt%, only 33% of the compositions are in Fe/Mg equilibrium. Hbl-glass $^{Fe/Mg}Kd$ values span a narrower range of values, from 0.04 to 0.7 (Figure 7). The majority of these Hbl compositions (57%) are in Fe/Mg equilibrium with their associated glasses, which are primarily rhyolitic in composition. It is noteworthy that the disequilibrium $^{Fe/Mg}Kd$ values between Hbl and bulk-rock from plutonic and volcanic samples is typically restricted to values greater than, not

less than, that of the nominal equilibrium range (i.e. are > 0.43), which suggests that Hbl in these samples is too Fe-rich (too evolved) to be in equilibrium with melt of host-rock composition. In contrast, disequilibrium $^{Fe/Mg}Kd$ values between Hbl and glass is primarily $<$ 0.13, which suggests that Hbl in these samples is too Mg-rich (too primitive) to be in equilibrium with the glass.

Hornblende Chemometry

The Al-in-Hbl barometer has seen wide usage since its original conception (Hammarstrom and Zen, 1986) and subsequent modifications. However, the use of Hbl as a barometer appears to be highly restricted (e.g. Hollister et al., 1987; Anderson and Smith, 1995) due to Al-in-Hbl being more sensitive to temperature and Al_2O_3 content of the melt than to pressure (Molina et al., 2015; Putirka, 2016a). The recognition that Hbl compositional variability is primarily related to changes in temperature and melt composition has since brought about the development of a number of equations that relate Hbl major element compositions to temperature and anhydrous melt compositions (Ridolfi et al., 2010; Ridolfi and Renzulli, 2012; Molina, 2015; Putirka, 2016a; Zhang et al., 2017). Hornblende chemometry is based on multivariate least-squares regression analysis of Hbl and glass compositions along with pressure, temperature, and fO_2 data from experimental studies (Ridolfi and Renzulli, 2012; Putirka, 2016a; Zhang et al., 2017). The first comprehensive series of chemometric equations for calculating equilibrium melt SiO_2, TiO_2, Al_2O_3, FeO, MgO, CaO, and K_2O were published by Ridolfi and Renzulli (2012), however, these equations rely on pressure estimates. Zhang et al. (2017) developed a series of chemometric equations which are independent of pressure and allow for an estimation of anhydrous equilibrium melt compositions for SiO_2, TiO_2, Al_2O_3, FeO, MgO, CaO,

346 and K_2O. Given that the uncertainties of pressure estimates are variably constrained for each of
347 the plutonic and volcanic systems investigated here, we utilize the equations of Zhang et al.
348 (2017).

349 Comparisons between the calculated melt and plutonic bulk-rock compositions are
350 presented in Figure 8. In most cases, there is limited or no correlation between bulk-rock
351 compositions and the results of the chemometric calculations. For example, > 95% of Hbl
352 analyses yield calculated melt compositions that are more evolved (i.e. higher SiO_2 and lower
353 MgO, FeO, and CaO) than the bulk-rock composition. Some Hbl from Mt Stuart, Black Peak,
354 Tenpeak, and Wooley Creek support crystallization from intermediate melt compositions.
355 However, 84% of the plutonic Hbl data yield calculated melt SiO_2 values > 70 wt%, 76% of
356 analyses yield calculated melt CaO < 3 wt%, and 96% of analyses yield calculated melt MgO <
357 1wt%. Thus, the bulk compositions of these plutonic rocks is typically more mafic, and in some
358 cases significantly more mafic, than the calculated melts in equilibrium with Hbl analyzed from
359 these rocks.

360 Comparisons of volcanic bulk-rock and glass compositions with melts calculated using
361 Hbl chemometry are presented in Figures 9 and 10, respectively. The calculated melt SiO_2 from
362 Hbl in volcanic systems varies from 41–78 wt% for 95% of the analyses. Only 55% of these
363 estimated melt compositions are in equilibrium with their host bulk-rock SiO_2 composition,
364 although 70% are in equilibrium with their host glass SiO_2 composition. Where spatial
365 information (core and rim) exists for Hbl analyses, a similar proportion of the rims (70%) are in
366 equilibrium with their host glass SiO_2 composition (Supplementary Figure 4). In the cases where
367 estimated melt compositions are not similar to the host glass compositions, the majority (> 96%)
368 of estimated melts have lower SiO_2 contents than the existing glass. In contrast, comparison of

369 estimated melts with bulk-rock compositions show that the estimated melts are more silicic than
370 the host rock for 89% of analyses that are in disequilibrium.

371 In summary, for plutons, the majority of bulk-rock compositions are more mafic than
372 calculated melt compositions. For volcanic rocks, some of the calculated melt compositions are
373 similar to bulk-rock and glass compositions, although, many calculated melt compositions are
374 more evolved than the bulk-rocks, but less evolved than groundmass glass compositions.
375

376 **DISCUSSION**
377

378 **Textural and Compositional Modification of Hornblende in Plutons**

379 The extent to which Hbl from the TIC experienced textural and compositional
380 modification is controversial (e.g. Barnes et al., 2016c; Challener and Glazner 2017). Challener
381 and Glazner (2017) cite the long durations over which TIC minerals were held at greenschist to
382 amphibolite facies temperatures and argue that the inclusion rich assemblages preserved in Hbl
383 are products of closed system metamorphic reactions involving the original Hbl. Thus, the
384 original Hbl is interpreted to have undergone significant textural and compositional modification
385 such that only remnants of the original magmatic Hbl is preserved. There are at least three
386 important textural and compositional arguments cited by Challener and Glazner (2017) in favor
387 of these interpretations. First, they argue that textural evidence supporting magmatic growth (e.g.
388 concentric zoning) is absent and that irregular patchy zoning requires multiple growth events.
389 Second, they point out that inclusions are abundant in Hbl phenocrysts (up to 45%), and that
390 some inclusion assemblages are evidence of crystallization at greenschist-facies temperature
391 conditions (i.e. albite, chlorite, actinolite, ± clinozoisite). Last, they suggest that the bulk

composition of the observed Hbl + inclusions can be described by a reaction product of some combination of high-Al Hbl with 5-30% biotite, proposing that recrystallization occurred within the closed system capsule of the original igneous Hbl. In contrast, Barnes et al. (2016c) proposed that compositional zoning in Hbl is common and that this zoning reflects changes in magma composition. Their arguments are based on the occurrence of core to rim compositional zoning patterns, the co-variation of fast- and slow-diffusing trace elements (e.g. Sr and Ba versus REE), calculated temperatures of crystallization that are representative of magmatic conditions, and on the preservation of compositionally distinct Hbl populations within individual samples. Barnes et al. (2016c) also recognize patches of blue–green actinolitic amphibole in some Hbl and interpret these zones as products of near-solidus to subsolidus replacement of olive-colored Hbl.

Patchy zoning is common in Hbl from the TIC, however, as indicated by Barnes et al. (2016c) its occurrence is not necessarily ubiquitous. Inclusion assemblages and the proportion of inclusions also vary widely, even within large euhedral Hbl phenocrysts. Given that patchy zoning, inclusion assemblages, and inclusion proportions vary within and between samples, we suggest that bulk diffusive resetting of individual Hbl is unlikely and that patchy zoning instead develops through a localized process. Furthermore, the preservation of magmatic crystallization histories in Hbl from the TIC is supported in some Hbl by regular zoning patterns, co-variation of both fast- and slow-diffusing trace elements (Barnes et al., 2016c), magmatic textures such as rare concentric zoning, magmatic crystallization temperatures, and compositional overlap with Hbl from volcanic systems. This conclusion does not preclude the effects of late-stage magmatic alteration, which is to be expected in plutons that crystallized from hydrous magmas.

Patchy zoning in Hbl from the TIC is interpreted here as a product of dissolution-reprecipitation at near-solidus to subsolidus conditions, whereby high-Al Hbl is replaced by low-

Al Hbl. Dissolution of high-Al magnesiohornblende and reprecipitation of low-Al magnesiohornblende or actinolite leads to a decrease in molar volume (Okamoto and Toriumi, 2005; Challener and Glazner, 2017) and therefore an increase in porosity that allows for melt and/or fluids to stay in contact with dissolution fronts (Putnis, 2002, 2009). Textural observations agree with this interpretation. For example, the boundaries between high-Al and low-Al Hbl is commonly sharp and rounded, suggestive of dissolution processes. Furthermore, the high-Al and low-Al Hbl appear to share the same crystal lattice, at least optically (e.g. similar extinction angles). This suggests that an epitaxial relationship exists between the two zones, consistent with pseudomorphic replacement and coupled dissolution-reprecipitation reactions (Putnis, 2002; 2009). Dissolution-reprecipitation is also supported by the occurrence of a compositional gap at ~ 740–760°C or at ~ 7.2–7.4 Si (apfu) in Hbl from most samples (e.g. Figure 4). Small variations in the maximum temperatures over which patchy zoning develops could be a function of the temperatures at which a fluid phase developed in individual magma batches. Note that Hbl with calculated temperatures below 750°C is rarely present as Hbl rims or as texturally homogeneous Hbl, but is instead from patchy zones. Hornblende rims and Hbl that appears texturally homogenous at the petrographic scale typically yield temperatures above 750°C. Therefore, Hbl growth at near-solidus conditions primarily occurs via replacement reactions.

The proportion of Hbl with calculated temperatures < 750°C in the TIC is ~ 26% and Hbl with temperatures < 650°C is << 1%. If the other plutonic systems investigated in this study are also considered, the proportion of Hbl with temperatures < 750°C is < 24% and Hbl with temperatures < 650°C is < 1%. Thus, the majority Hbl analyzed from plutonic systems records information about magmatic conditions that is comparable to conditions preserved in Hbl from volcanic systems. We therefore suggest that with detailed petrographic and analytical study of a

representative suite of samples, it is possible to identify local modification of Hbl compositions by super-solidus to sub-solidus dissolution-reprecipitation as well as by sub-solidus, lower-T deuteric alteration.

Mineral-Melt Disequilibrium and Evidence of Crystal Accumulation

The petrogenetic relationship between silicic plutonic and volcanic systems is still unclear (e.g. Read, 1957; Buddington, 1959; Lipman, 1984, 2007; Bachmann and Bergantz, 2004; Hildreth, 2004; Bachmann et al., 2007; Coleman et al., 2012; Lipman and Bachmann, 2015; Glazner et al., 2018). Authors in favor of a petrogenetic link cite the spatial and temporal proximity between many plutonic and volcanic systems (Lipman, 2007; Lipman and Bachmann, 2015; Watts et al., 2016), the occurrence of negative gravity anomalies (suggestive of silicic batholiths) beneath some large-volume ignimbrites (Lipman 2007; Lipman and Bachmann, 2015), and the complementary relationship between silicic plutonic and volcanic rocks (e.g. Gelman et al., 2014; Lee and Morton, 2015). However, the recognition that plutons may be assembled incrementally over millions of years, with low average magma addition rates, has led some authors (e.g. Coleman et al., 2004; Glazner et al., 2004; Glazner et al., 2018) to suggest that plutons and large-volume ignimbrites are not genetically linked and by extension of these arguments, that magma chambers that are capable of crystal-liquid separation, mixing, assimilation, and recycling of material are not important in the middle to upper crust. If magma differentiation is restricted to lower crustal hot zones (Annen et al., 2006) and plutons are assembled incrementally through low magma addition rates without producing magma bodies capable of in-situ differentiation, then crystal accumulation and melt loss should not be prevalent within upper crustal plutonic systems. Alternatively, if magma addition rates are high, allowing

461 for extensive magma bodies to form and differentiate at the site of emplacement and for
462 connections between volcanic and plutonic systems to occur, then crystal accumulation and melt
463 loss should be important magmatic processes. Hornblende-melt $^{Fe/Mg}$Kd tests and Hbl-
464 chemometry provide ways in which individual samples can be evaluated for crystal accumulation
465 and melt loss effects.

466 Hornblende from the seven plutonic systems (Tuolumne, Wooley Creek, English Peak,
467 Ashland, Tenpeak, Black Peak, and Mt Stuart) investigated in this study is only rarely in
468 compositional equilibrium with host bulk-rock compositions (Figure 8). Instead, bulk-rock
469 compositions are typically too Mg-rich on the basis of Hbl-melt $^{Fe/Mg}$Kd tests and too mafic
470 compared to melts calculated from Hbl-chemometry. The calculated melts are mostly rhyolitic,
471 with few analyses yielding intermediate melt compositions (Figure 8). These calculated rhyolitic
472 melts do not represent low temperature differentiates given that 90% of the Hbl analyses reported
473 here yield calculated crystallization temperatures above 780°C. Furthermore, plagioclase
474 compositions from these plutons also support evolved melt compositions. For example, the
475 maximum and minimum anorthite content of plagioclase in samples where Hbl was a primary
476 rather than peritectic phase ranges from: An_{57}–An_{12} in the Wooley Creek batholith (Barnes,
477 1983); An_{53}–An_{19} in the English Peak pluton (Barnes et al., 2016a); and An_{42}–An_{9} in the
478 Tuolumne Intrusive Complex (Bateman and Chappell, 1979; Barnes et al., 2016c). Note that the
479 calculated melt compositions generally show a narrow range of values regardless of the range in
480 bulk-rock compositions (Figure 8). Thus, the compositional variability of these plutonic bulk-
481 rock samples seems to be dominated by varying extents of crystal accumulation and/or melt loss
482 rather than to a diversity of melt compositions. The general absence of calculated intermediate
483 melt compositions in plutons agrees with melt inclusion studies from arc volcanic rocks, which

484 indicate that melt compositions are largely bimodal, with peaks at 54 and 76 wt% SiO_2 (Reubi
485 and Blundy, 2009). Melt loss from these intrusive systems potentially results from a variety of
486 processes such as hindered settling, compaction, gas-filter pressing, and/or regional deformation,
487 although, the ways in which the relative importance of these processes can be deciphered from
488 individual plutonic systems is uncertain (Holness, 2018). Regardless of the processes by which
489 melt escapes, the result is either that these silicic melts are redistributed in the crust (e.g. silicic
490 dikes or plutons) or that the melts escape subcrustal reservoirs and erupt. Detailed mass-balance
491 studies that consider the effects of crystal accumulation and melt loss on bulk-rock compositions
492 are needed in order first to quantify the volumes of silicic melt that are lost from these plutonic
493 systems (e.g. Barnes et al., 2016a; Barnes et al., in revision) and second to determine the
494 proportion of melt that is redistributed in the crust versus the proportion that has escaped through
495 volcanic eruption. It should be noted that the dissolution-reprecipitation processes discussed
496 above coupled with the likelihood of crystal accumulation and/or melt loss present additional
497 challenges to the application of Al-in-Hbl barometry. For example, in Hbl from the TIC and
498 English Peak pluton (Barnes et al., 2017), the majority of Hbl growth at near-solidus conditions
499 is related to dissolution-reprecipitation reactions. Therefore, in cumulate samples where low
500 temperature melt has escaped and/or where low temperature dissolution-reprecipitation processes
501 did not operate, pressure estimates will be restricted to higher temperature Hbl and therefore lead
502 to higher pressure estimations (cf. Putirka, 2016a).

503 In volcanic systems, Hbl in dacitic to rhyolitic samples is more likely to be in Fe-Mg
504 equilibrium compared to Hbl from more mafic and intermediate rocks (Figure 9). As with the
505 plutonic rocks, in cases where calculated melts are dissimilar to bulk-rock compositions, the
506 calculated melts are typically more evolved, but note that volcanic glasses that are not in

equilibrium with Hbl are instead typically too evolved (Figure 10). The differences between calculated melts and the rhyolitic glasses is commonly minor such that the Hbl may have originated from a less fractionated melt, although in some cases (e.g. in intermediate bulk-rock samples) the differences between the calculated melts and glass compositions is significant and may indicate the occurrence of mixed crystal populations. For dacitic to rhyolitic bulk-rock samples, the variability observed between bulk-rock and calculated melt SiO_2 is small and could therefore be attributable to either melt fractionation or to small amounts of crystal accumulation. However, bulk-rock compositions and calculated melts may both vary by > 20 wt% SiO_2 for the more mafic and intermediate bulk-rock samples. Thus, either extreme fractional crystallization is recorded in these Hbl or these wide variations in SiO_2 instead reflect magma mixing between mafic and silicic magmas. Magma mixing seems plausible given that calculated melt SiO_2 compositions from individual samples (e.g. Redoubt) is bimodal in some cases (Coombs et al., 2013). It is noteworthy that there is a general absence of lower temperature (< 750°C) Hbl from volcanic systems. The absence of lower temperature Hbl is consistent with the idea that magmatic mushes at temperatures lower than 750°C are unlikely to erupt. In a more complex scenario, if magmas that cooled below 750°C were reheated and then erupted, then evidence for dissolution of low T Hbl is expected.

IMPLICATIONS

The preservation of magmatic conditions in Hbl from plutons allows for Hbl – melt $^{Fe/Mg}Kd$ tests (Putirka, 2016a) and Hbl chemometry (Ridolfi and Renzulli, 2012; Putirka, 2016a; Zhang et al., 2017) to be used to both assess the significance of crystal accumulation and/or melt loss processes (in conjunction with other magmatic processes) and to determine equilibrium melt

compositions. This work indicates that melts from which Hbl crystallized in quartz-bearing plutons in the mid- to upper-crust are generally rhyolitic in composition and that bulk-rock diversity in these plutons is dominated by varying extents of crystal accumulation and/or melt loss. Hornblende from more mafic to intermediate volcanic systems instead yield wide ranges of calculated melt compositions, which in some samples display bimodality between mafic and silicic melts. Thus, many of the more mafic to intermediate bulk-rock samples investigated in this study are likely products of magma mixing. If the petrogenetic links between plutonic and volcanic rocks is to be understood and quantified, then detailed assessment and analysis of crystal accumulation and melt loss processes is needed from individual magmatic systems. It will also be critically important to identify the mechanisms by which evolved melts escape from magmatic mushes (e.g., Bachmann and Huber, 2018; Holness, 2018). This task will require individual case studies that focus on plutonic rock textures, rock and mineral compositions, and modeling of melt compositions and physical properties.

ACKNOWLEDGEMENTS

This work was supported by NSF EAR grants awarded to Barnes (EAR 155509), Memeti (EAR 1550935), and Paterson (EAR 1250219 and EAR 1624847). We thank George Morgan, Melanie Barnes, and Jake Sullivan for their assistance in the laboratory. The manuscript was greatly improved by reviews from Phil Piccoli, Charlotte Allen, and an anonymous reviewer and editorial comments from Jade Star Lackey.

551 **REFERENCES**

552 Anderson, J. L. and Smith., D.R. (1995). The effects of temperature and f_{O2} on the Al-in-
553 hornblende barometer. *American Mineralogist* **80**, 549-559.
554 Allan, A. S. R., Barker, S. J., Millet, M.-A., Morgan, D. J., Rooyakkers, S. M., Schipper, C. I.
555 and Wilson, C. J. N. (2017). A cascade of magmatic events during the assembly and
556 eruption of a super-sized magma body. Contributions to Mineralogy and Petrology 172,
557 49.
558 Annen, C., Blundy, J.D., and Sparks, J. (2006). The Genesis of Intermediate and Silicic Magmas
559 in Deep Crustal Hot Zones. Journal of Petrology 47, 505-539.
560 Bachmann, O. and Bergantz, G. W. (2004). On the Origin of Crystal-poor Rhyolites: Extracted
561 from Batholithic Crystal Mushes. Journal of Petrology 45, 1565-1582.
562 Bachmann, O. and Bergantz, G. W. (2008). Rhyolites and their Source Mushes across Tectonic
563 Settings. Journal of Petrology 49, 2277-2285.
564 Bachmann, O., and Dungan, M.A. (2002). Temperature-induced Al-zoning in hornblendes of the
565 Fish Canyon magma, Colorado. American Mineralogist 87, 1062-1076.
566 Bachmann, O., Dungan. M.A., and Lipman, P.W. (2002). The Fish Canyon Magma Body, San
567 Juan Volcanic Field, Colorado: Rejuvenation and Eruption of an Upper-Crustal Batholith.
568 Journal of Petrology 43, 1469-1503.
569 Bachmann, O., and Huber, C. (2018). The inner workings of crustal distillation columns; the
570 physical mechanisms and rates controlling phase separation in silicic magma reservoirs.
571 Journal of Petrology, doi/10.1093/petrology/egy103/5184274.

572 Bachmann, O., Miller, C. F. and de Silva, S. L. (2007). The volcanic–plutonic connection as a
573 stage for understanding crustal magmatism. Journal of Volcanology and Geothermal
574 Research 167, 1-23.
575 Barnes, C. G. (1983). Petrology and Upward Zonation of the Wooley Creek Batholith, Klamath
576 Mountains, California. Journal of Petrology 24, 495-537.
577 Barnes, C.G. (1987). Mineralogy of the Wooley Creek Batholith, Slinkard Pluton, and related
578 dikes, Klamath Mountains, Northern California. American Mineralogist 72, 879-901.
579 Barnes, C. G., Berry, R., Barnes, M. A. and Ernst, W. G. (2017). Trace element zoning in
580 hornblende: Tracking and modeling the crystallization of a calc-alkaline arc pluton.
581 American Mineralogist 102, 2390-2405.
582 Barnes C. G., Coint, N. and Yoshinobu, A. (2016a). Crystal accumulation in a tilted arc
583 batholith. American Mineralogist, 1719.
584 Barnes, C. G., Ernst, W. G., Berry, R. and Tsujimori, T. (2016b). Petrology and Geochemistry of
585 an Upper Crustal Pluton: a view into Crustal-scale Magmatism during Arc to Retro-arc
586 Transition. Journal of Petrology 57, 1361-1388.
587 Barnes, C. G., Memeti, V. and Coint, N. (2016c). Deciphering magmatic processes in calc-
588 alkaline plutons using trace element zoning in hornblende. American Mineralogist 101,
589 328-342.
590 Barnes, C.G., Werts, K., Memeti, V. and Ardill, K. (in revision). Most granitoid rocks are
591 cumulates: deductions from hornblende compositions and zircon saturation. Journal of
592 Petrology.
593 Bateman, P. C. (1992). Plutonism in the Central Part of the Sierra Nevada Batholith, California.
594 U.S. Geological Survey Professional Paper 1483, 1-186.

595 Bateman, P. C., and Chappel, B.W. (1979). Crystallization, fractionation, and solidification of
596 the Tuolumne Intrusive Series, Yosemite National Park, California. Geological Society of
597 America Bulletin 90, 465-482.
598 Berry, R.A. (2015) Hornblende as an indicator of magma batches and magmatic processes in the
599 English Peak pluton, Klamath Mountains, California. M.S. thesis, Texas Tech University,
600 Lubbock, 201
601 Bowen, N.L. (1928). The Evolution of the Igneous Rocks. Princeton University Press. Princeton,
602 NJ.
603 Buddington, A. F. (1959). Granite Emplacement With Special Reference to North America. GSA
604 Bulletin 70, 671-747.
605 Challener, S. C. and Glazner, A. F. (2017). Igneous or metamorphic? Hornblende phenocrysts as
606 greenschist facies reaction cells in the Half Dome Granodiorite, California. American
607 Mineralogist 102, 436-444.
608 Chambefort, I., Dilles, J. H. and Longo, A. A. (2013). Amphibole Geochemistry of the
609 Yanacocha Volcanics, Peru: Evidence for Diverse Sources of Magmatic Volatiles
610 Related to Gold Ores. Journal of Petrology 54, 1017-1046.
611 Chan, C. F., Shea, E. K., Kent, A. J., Miller, R. B., Miller, J. S., and Bowring, S. A. (2017)
612 Formation of a sheeted intrusive complex within the deep-crustal Tenpeak pluton, North
613 Cascades, Washington. Geosphere, 13, 5, 1610-1639.
614 Christiansen, E. H. and McCurry, M. (2008). Contrasting origins of Cenozoic silicic volcanic
615 rocks from the western Cordillera of the United States. Bulletin of Volcanology 70, 251-
616 267.

Coint, N., Barnes, C.G., Yoshinobu, A.S., Barnes, M.A., Buck, S. (2013b). Use of trace element abundances in augite and hornblende to determine the size, connectivity, timing, and evolution of magma batches in a tilted batholith. Geosphere 9, 1747-1765.

Coint, N., Barnes, C.G., Yoshinobu, A.S., Chamberlain, K.R., Barnes, M.A. (2013a). Batch-wise assembly and zoning of a tilted calc-alkaline batholith: Field relations, timing, and compositional variation. Geosphere 9, 1729-1746.

Coleman, D. S., Gray, W., Glazner, A.F. (2004). Rethinking the emplacement and evolution of zoned plutons: Geochronologic evidence for incremental assembly of the Tuolumne Intrusive Suite, California. Geological Society of America 32, 433-436.

Coleman, D. S., Bartley, J.M., Glazner, A.F., Pardue, M.J. (2012). Is chemical zonation in plutonic rocks driven by changes in source magma composition or shallow-crustal differentiation? Geosphere 8, 1568-1587.

Collins, W., Wiebe, R., Healy, B. and W. Richards, S. (2006). Replenishment, Crystal Accumulation and Floor Aggradation in the Megacrystic Kameruka Suite, Australia.

Coombs, M. L., Sisson, T. W., Bleick, H. A., Henton, S. M., Nye, C. J., Payne, A. L., Cameron, C. E., Larsen, J. F., Wallace, K. L. and Bull, K. F. (2013). Andesites of the 2009 eruption of Redoubt Volcano, Alaska. Journal of Volcanology and Geothermal Research 259, 349-372.

Davidson, J., Tepley, F., III, Palacz, Z. and Meffan-Main, S. (2001). Magma recharge, contamination and residence times revealed by in situ laser ablation isotopic analysis of feldspar in volcanic rocks. Earth and Planetary Science Letters 184, 427–442.

638 Davis, J. W., Coleman, D. S., Gracely, J. T., Gaschnig, R. and Stearns, M. (2012). Magma
639 accumulation rates and thermal histories of plutons of the Sierra Nevada batholith, CA.
640 Contributions to Mineralogy and Petrology 163, 449-465.
641 De Angelis, S. H., Larsen, J. and Coombs, M. (2013). Pre-eruptive Magmatic Conditions at
642 Augustine Volcano, Alaska, 2006: Evidence from Amphibole Geochemistry and
643 Textures. Journal of Petrology 54, 1939-1961.
644 DePaolo, D. J. (1981). Trace element and isotopic effects of combined wallrock assimilation and
645 fractional crystallization. Earth and Planetary Science Letters 53, 189-202.
646 Deering, C. D. (2009). Cannibalization of an amphibole-rich andesitic progenitor induced by
647 caldera-collapse during the Matahina eruption: Evidence from amphibole compositions.
648 American Mineralogist 94, 1162-1174.
649 Deering, C. D., Bachmann, O. (2010). Trace element indicators of crystal accumulation in silicic
650 igneous rocks. Earth and Planetary Science Letters 297, 324-331.
651 Deering, C. D., Cole, J. W., and Vogel, T. A. (2011). Extraction of crystal-poor rhyolite from a
652 hornblende-bearing intermediate mush: a case study of the caldera-forming Matahina
653 eruption, Okataina volcanic complex. Contributions to Mineralogy and Petrology 161,
654 129-151.
655 Druitt, T. H. and Bacon, C. R. (1989). Petrology of the zoned calc alkaline magma chamber of
656 Mount Mazama, Crater Lake, Oregon. Contributions to Mineralogy and Petrology 101,
657 245-259.
658 Esawi, E. K. (2004). AMPH-CLASS: An Excel spreadsheet for the classification and
659 nomenclature of amphiboles based on the 1997 recommendations of the International
660 Mineralogical Association. Computers and Geosciences 30, 753-760.

661 Gelman, S. E., Deering, C. D., Bachmann, O., Huber, C. and Gutiérrez, F. J. (2014). Identifying
662 the crystal graveyards remaining after large silicic eruptions. Earth and Planetary Science
663 Letters 403, 299-306.
664 Glazner, A.F., Bartley, J.M., Coleman, D.S., Gray, W., and Taylor, R.Z., (2004). Are plutons
665 assembled over millions of years by amalgamation from small magma chambers?: GSA
666 Today, 14, 4–11.
667 Glazner, A., Coleman, D., and Mills, R. (2018). The Volcanic-Plutonic Connection. Springer
668 Berlin Heidelberg, 1-22.
669 Gorbach, N. V. and Portnyagin, M. V. (2011). Geology and petrology of the lava complex of
670 Young Shiveluch Volcano, Kamchatka. Petrology 19, 134.
671 Gribble, R. F., Barnes, C. G., Donato, M. M., Hoover, J. D. and Kistler, R. W. (1990).
672 Geochemistry and Intrusive History of the Ashland Pluton, Klamath Mountains,
673 California and Oregon. Journal of Petrology 31, 883-923.
674 Hammarstrom, J. M., Zen, E-an. (1986). Aluminum in hornblende: An empirical igneous
675 geobarometer. American Mineralogist 71, 1297-1313.
676 Hawthorne, F. C., Oberti, R., Harlow, G. E., Maresch, W. V., Martin, R. F., Schumacher, J. C.
677 and Welch, M. D. (2012). Nomenclature of the amphibole supergroup. American
678 Mineralogist 97, 2031-2048.
679 Hepeng, T. (2016). Using hornblende geochemistry to unravel the emplacement of magmatic
680 structures, Tuolumne Intrusive Complex, California [MS Thesis]: Lubbock, Texas Tech
681 University, 1-99.

682 Hildreth, W. (2004). Volcanological perspectives on Long Valley, Mammoth Mountain, and
683 Mono Craters: several contiguous but discrete systems. Journal of Volcanology and
684 Geothermal Research 136, 169-198.
685 Hildreth, W. and Moorbath, S. (1988). Crustal contributions to arc magmatism in the Andes of
686 Central Chile. Contributions to Mineralogy and Petrology 98, 455-489.
687 Hollister, L. S., Grissom, G.C., Peters, E.K., Stowell, H.H., and Sisson, V.B. (1987).
688 Confirmation of the empirical correlation of Al in hornblende with pressure of
689 solidification of calc-alkaline plutons. American Mineralogist 72, 231-239.
690 Holness, M. B. (2018). Melt segregation from silicic crystal mushes: a critical appraisal of
691 possible mechanisms and their microstructural record. Contributions to Mineralogy and
692 Petrology 173, 48.
693 Keller, C.B., Schoene, B., Barboni, M., Samperton, K.M., and Husson, J.M. (2015) Volcanic–
694 plutonic parity and the differentiation of the continental crust. Nature, 523, 301–307.
695 Klaver, M., Blundy, J. D. and Vroon, P. Z. (2017). Generation of arc rhyodacites through
696 cumulate-melt reactions in a deep crustal hot zone: Evidence from Nisyros volcano. Earth
697 and Planetary Science Letters 497, 169-180.
698 Larsen, J. F., Nye, C. J., Coombs, M. L., Tilman, M., Izbekov, P. and Cameron, C. (2010).
699 Petrology and geochemistry of the 2006 eruption of Augustine Volcano: Chapter 15 in
700 The 2006 eruption of Augustine Volcano, Alaska. In: Power, J. A., Coombs, M. L. and
701 Freymueller, J. T. (eds.) Professional Paper, 335-382.
702 Leake, B. E., Woolley, A.R., Arps, C.E.S., Birch, W.D., Gilbert, M.C., Grice, J.D., Hawthorne,
703 F.C., Kato, A., Kisch, H.J., Krivovichev, V.G., Linthout, K., Laird, J., Mandarino, J.A.,
704 Maresch, W.V., Nickel, E.H., Rock, N.M.S., Schumacher, J.C., Smith, D.C., Stephenson,

N.C.N., Ungaretti, L., Whittaker, E.J.W., Youzhi, G. (1997). Nomenclature of Amphiboles: Report of the subcommittee on amphiboles of the international mineralogical association, commission on new minerals and mineral names. The Canadian Mineralogist 35, 219-246.

Lee, C.-T. A. and Morton, D. M. (2015). High silica granites: Terminal porosity and crystal settling in shallow magma chambers. Earth and Planetary Science Letters 409, 23-31.

Lee, C.-T. A., Morton, D. M., Farner, M. J. and Moitra, P. (2015). Field and model constraints on silicic melt segregation by compaction/hindered settling: The role of water and its effect on latent heat release. American Mineralogist 100, 1762-1777.

Lipman, P. W. (1984). The roots of ash flow calderas in western North America: Windows into the tops of granitic batholiths. Journal of Geophysical Research: Solid Earth 89, 8801-8841.

Lipman, P. W. (2007). Incremental assembly and prolonged consolidation of Cordilleran magma chambers: Evidence from the Southern Rocky Mountain volcanic field. Geosphere 3, 42-70.

Lipman, P. W. and Bachmann, O. (2015). Ignimbrites to batholiths: Integrating perspectives from geological, geophysical, and geochronological data. Geosphere 11, 705-743.

McCarthy, T. S. and Hasty, R. A. (1976). Trace element distribution patterns and their relationship to the crystallization of granitic melts. Geochimica et Cosmochimica Acta 40, 1351-1358.

Memeti, V., Paterson, S., Mundil, R. (2014). Day 4: Magmatic evolution of the Tuolumne Intrusive Complex. Geological Society of America Field Guide 34, 43-74.

727 Miller, C. F., Furbish, D. J., Walker, B. A., Claiborne, L. L., Koteas, G. C., Bleick, H. A. and
728 Miller, J. S. (2011). Growth of plutons by incremental emplacement of sheets in crystal-
729 rich host: Evidence from Miocene intrusions of the Colorado River region, Nevada, USA.
730 Tectonophysics 500, 65-77.
731 Molina, J. F., Moreno, J. A., Castro, A., Rodríguez, C. and Fershtater, G. B. (2015). Calcic
732 amphibole thermobarometry in metamorphic and igneous rocks: New calibrations based
733 on plagioclase/amphibole Al-Si partitioning and amphibole/liquid Mg partitioning. Lithos
734 232, 286-305.
735 Nakada, S., Bacon, C. R. and Gartner, A. E. (1994). Origin of Phenocrysts and Compositional
736 Diversity in Pre-Mazama Rhyodacite Lavas, Crater Lake, Oregon. Journal of Petrology
737 35, 127-162.
738 Pallister, J. S., Thornber, C. R., Cashman, K. V., Clynne, M. A., Lowers, H., Mandeville, C. W.,
739 Brownfield, I. K. and Meeker, G. P. (2008). Petrology of the 2004-2006 Mount St.
740 Helens lava dome -- implications for magmatic plumbing and eruption triggering. In:
741 Sherrod, D. R., Scott, W. E. and Stauffer, P. H. (eds.) Professional Paper. Reston, VA,
742 647-702.
743 Paterson, S. R., Okaya, D., Memeti, V., Economos, R., Miller, R.B. (2011). Magma addition and
744 flux calculations of incrementally constructed magma chambers in continental margin
745 arcs: Combined field, geochronologic, and thermal modeling studies. Geosphere 7, 1439-
746 1468.
747 Paterson, S., Memeti, V., Mundil, R. and Žák, J. (2016). Repeated, multiscale, magmatic erosion
748 and recycling in an upper-crustal pluton: Implications for magma chamber dynamics and
749 magma volume estimates. American Mineralogist 101, 2176-2198.

Putnis, A. (2002). Mineral replacement reactions: from macroscopic observations to microscopic mechanisms. Mineralogical Magazine 66, 689-708.

Putnis, A. (2009). Mineral Replacement Reactions. Reviews in Mineralogy and Geochemistry 70, 87-124.

Putirka, K. D. (2008). Thermometers and Barometers for Volcanic Systems. Reviews in Mineralogy and Geochemistry 69, 61-120.

Putirka, K. (2016a). Amphibole thermometers and barometers for igneous systems and some implications for eruption mechanisms of felsic magmas at arc volcanoes. American Mineralogist 101, 841-858.

Putirka, K. (2016b). Rates and styles of planetary cooling on Earth, Moon, Mars, and Vesta, using new models for oxygen fugacity, ferric-ferrous ratios, olivine-liquid Fe-Mg exchange, and mantle potential temperature. American Mineralogist 101, 819-840.

Ratschbacher, B. C., Keller, C. B., Schoene, B., Paterson, S. R., Anderson, J. L., Okaya, D., Putirka, K. and Lippoldt, R. (2018). A New Workflow to Assess Emplacement Duration and Melt Residence Time of Compositionally Diverse Magmas Emplaced in a Sub-volcanic Reservoir. Journal of Petrology 59, 1787-1809.

Read, H. H. (1957). The Granite Controversy. Geologiska Föreningen i Stockholm Förhandlingar 79, 591-593.

Reid, J. B., Jr., Evans, O. C. and Fates, D. G. (1983). Magma mixing in granitic rocks of the central Sierra Nevada, California. Earth and Planetary Science Letters 66, 243-261

Reubi, O. and Blundy, J. (2009). A dearth of intermediate melts at subduction zone volcanoes and the petrogenesis of arc andesites. Nature 461, 1269.

772 Ridolfi, F. and Renzulli, A. (2012). Calcic amphiboles in calc-alkaline and alkaline magmas:
773 thermobarometric and chemometric empirical equations valid up to 1,130°C and 2.2 GPa.
774 Contributions to Mineralogy and Petrology 163, 877-895.
775 Ridolfi, F., Renzulli, A. and Puerini, M. (2010). Stability and chemical equilibrium of amphibole
776 in calc-alkaline magmas: an overview, new thermobarometric formulations and
777 application to subduction-related volcanoes. Contributions to Mineralogy and Petrology
778 160, 45-66.
779 Roeder, P. L. and Emslie, R. F. (1970). Olivine-liquid equilibrium. Contributions to Mineralogy
780 and Petrology 29, 275-289.
781 Rooney, T. O., Franceschi, P. and Hall, C. M. (2011). Water-saturated magmas in the Panama
782 Canal region: a precursor to adakite-like magma generation? Contributions to Mineralogy
783 and Petrology 161, 373-388.
784 Rowe, M. C., Thornber, C. R. and Kent, A. J. R. (2008). Identification and evolution of the
785 juvenile component in 2004-2005 Mount St. Helens ash: Chapter 29 in A volcano
786 rekindled: the renewed eruption of Mount St. Helens, 2004-2006. In: Sherrod, D. R.,
787 Scott, W. E. and Stauffer, P. H. (eds.) Professional Paper. Reston, VA, 629-646.
788 Schaen, A. J., Singer, B. S., Cottle, J. M., Garibaldi, N., Schoene, B., Satkoski, A. M. and
789 Fournelle, J. (2018). Textural and Mineralogical Record of Low-pressure Melt Extraction
790 and Silicic Cumulate Formation in the Late Miocene Risco Bayo–Huemul Plutonic
791 Complex, Southern Andes. Journal of Petrology 59, 1991-2016.
792 Shane, P. and Smith, V. C. (2013). Using amphibole crystals to reconstruct magma storage
793 temperatures and pressures for the post-caldera collapse volcanism at Okataina volcano.
794 Lithos 156-159, 159-170.

795 Spera, F. J. and Bohrson, W. A. (2001). Energy-Constrained Open-System Magmatic Processes
796 I: General Model and Energy-Constrained Assimilation and Fractional Crystallization
797 (EC-AFC) Formulation. Journal of Petrology 42, 999-1018.
798 Thornber, C. R., Pallister, J. S., Lowers, H., Rowe, M. C., Mandeville, C. W. and Meeker, G. P.
799 (2008). Chemistry, mineralogy, and petrology of amphibole in Mount St. Helens 2004-
800 2006 dacite. In: Sherrod, D. R., Scott, W. E. and Stauffer, P. H. (eds.) Professional Paper.
801 Reston, VA, 727-754.
802 van Zalinge, M. E., Sparks, R. S. J. and Blundy, J. D. (2017). Petrogenesis of the Large-volume
803 Cardones Ignimbrite, Chile; Development and Destabilization of a Complex Magma–
804 Mush System. Journal of Petrology 58, 1975-2006.
805 Vernon, R. H. and Collins, W. J. (2011). Structural Criteria for Identifying Granitic Cumulates.
806 The Journal of Geology 119, 127-142.
807 Watts, K. E., John, D. A., Colgan, J. P., Henry, C. D., Bindeman, I. N. and Schmitt, A. K.
808 (2016). Probing the Volcanic–Plutonic Connection and the Genesis of Crystal-rich
809 Rhyolite in a Deeply Dissected Supervolcano in the Nevada Great Basin: Source of the
810 Late Eocene Caetano Tuff. Journal of Petrology 57, 1599-1644.
811 Weinberg, R. F. (2006). Melt segregation structures in granitic plutons. Geology 34, 305-308.
812 Wiebe, R. A. (1993). The Pleasant Bay Layered Gabbro—Diorite, Coastal Maine: Ponding and
813 Crystallization of Basaltic Injections into a Silicic Magma Chamber. Journal of Petrology
814 34, 461-489.
815 Wiebe, R. A., Blair, K. D., Hawkins, D. P. and Sabine, C. P. (2002). Mafic injections, in situ
816 hybridization, and crystal accumulation in the Pyramid Peak granite, California. GSA
817 Bulletin 114, 909-920

Žák, J. and Paterson, S. R. (2005). Characteristics of internal contacts in the Tuolumne Batholith, central Sierra Nevada, California (USA): Implications for episodic emplacement and physical processes in a continental arc magma chamber. Geological Society of America Bulletin 117, 1242-1255.

Zhang, J., Humphreys, M. C., Cooper, G. F., Davidson, J. P. and Macpherson, C. G. (2017). Magma mush chemistry at subduction zones, revealed by new melt major element inversion from calcic amphiboles. American Mineralogist 102, 1353-1367.

844 **Figure Captions**

845

846 **Figure 1**

847 Map of the Tuolumne Intrusive Complex after Memeti et al., 2014, modified by Katie Ardill with help
848 from Snir Attia. The map highlights the locations of Tuolumne Intrusive Complex samples that are
849 reported on in this study. Note that the sample numbers displayed on the map are all preceded by 'TLM'
850 in the data reported within Supplementary Data File 1.

851

852 **Figure 2**

853 Photomicrographs of hornblende from the Tuolumne Intrusive Complex illustrating complex patchy color
854 zoning (A,B) and concentric zoning (C). The dots and numbers in (A) correspond to individual electron
855 microprobe spot locations. **(a)** Hornblende with patchy color zoning from the equigranular Half Dome.
856 **(b)** Close up view of the white box from (A) highlighting the textural variability between the distinctly
857 colored zones. (**c**) Photomicrograph of a concentrically zoned Hornblende from the Tuolumne Intrusive
858 Complex. The orange dots represent individual electron microprobe spot locations and the values next to
859 each dot represent calculated crystallization temperatures (Putirka, 2016a).

860

861 **Figure 3**

862 Plot of hornblende Si vs $Mg/(Mg+Fe^{2+})$ for each of the lithological units of the Tuolumne Intrusive
863 Complex. The shaded fields encompass > 99% of the hornblende analyses from Kuna Crest (n = 204) and
864 equigranular Half Dome (n = 696). Note that there is significant compositional overlap between
865 hornblende from each of the units, although hornblende from Half Dome and Cathedral Peak is
866 commonly more magnesian than hornblende from Kuna Crest at low Si (apfu).

867

868 **Figure 4**

Plots of (**a**) Ti (apfu) vs Si (apfu) and (**b**) Ti (apfu) vs calculated temperature for the Half Dome Hornblende from Figure 2a. Note that the numbers correspond to the electron microprobe spot locations from Figure 2a.

Figure 5

Density contour plots of hornblende Si (apfu) vs major elements (Ti, Al, Mg, Na, K) and calculated temperature (Putirka, 2016a) for the twelve volcanic (red) and seven plutonic (blue) systems (see Table 1 for details). The four density contour levels reflect 100%, 75%, 50%, and 25% density intervals.

Figure 6

Histogram of volcanic and plutonic hornblende temperatures. Note the low temperature tail produced by hornblende from the plutonic systems and the high temperature peak (at ~ 950°C) produced by hornblende from the volcanic systems.

Figure 7

Bulk-rock SiO_2 vs Hbl-bulk-rock $^{Fe/Mg}Kd$ for (**a**) plutonic and (**b**) volcanic systems and (**c**) glass SiO_2 vs Hbl-glass $^{Fe/Mg}Kd$ for volcanic systems. The yellow boxes highlight the analyses that are in Fe/Mg equilibrium with their bulk-rock compositions. Note that Hbl is too Fe-rich to be in equilibrium with many of the plutonic and volcanic bulk-rocks and too Mg-rich to be in equilibrium with most glass compositions.

Figure 8

Bulk-rock vs calculated Hbl equilibrium melt compositions for plutonic systems. (**a**) SiO_2 (**b**) CaO (**c**) FeO and (**d**) K_2O. Equations 3, 7, 11, and 13 from Zhang et al., 2017 were used. Solid lines are 1:1 lines and dashed lines represent the errors associated with each of the chemometric equations.

Figure 9

Bulk-rock vs calculated Hbl equilibrium melt compositions for volcanic systems. (**a**) SiO_2 (**b**) CaO (**c**) FeO and (**d**) K_2O. Equations 3, 7, 11, and 13 from Zhang et al., 2017 were used. Solid lines are 1:1 lines and dashed lines represent the errors associated with each of the chemometric equations.

Figure 10

Volcanic glass vs calculated Hbl equilibrium melt compositions. (**a**) SiO_2 (**b**) CaO (**c**) FeO and (**d**) K_2O. Equations 3, 7, 11, and 13 from Zhang et al., 2017 were used. Solid lines are 1:1 lines and dashed lines represent the errors associated with each of the chemometric equations.

This is a preprint, the final version is subject to change, of the American Mineralogist (MSA)
Cite as Authors (Year) Title. American Mineralogist, in press.
DOI: https://doi.org/10.2138/am-2020-6972

Table 1. Summary of Hornblende, Bulk-Rock, and Glass Data

Location	Ref.	n	Bulk-Rock SiO_2 (wt%) *	Glass SiO_2 (wt%)*	Hbl Temperature (° C)	Avg Hbl Temp (° C)	Min Si (apfu)	Avg Si (apfu)	Min Ti (apfu)	Avg Ti (apfu)	% Act	% Ed	% Mg-Hs	% Mg-Hbl	% Prg	% Ts	Other
Cerro Patacon	1	279	58–59	n/a	854–973	934	5.97	6.23	0.13	0.18			29.7	0.4		69.9	
Fish Canyon	2,3	2060	68	77–78	754–959	800	6.18	6.95	0.1	0.15		7.0	2.8	89.1	1.0		
Mt St Helens	4,5	530	65	73–77	740–1016	909	5.93	6.43	0.05	0.25		0.4	15.1	16.6		67.9	
Redoubt	6	190	57–62	77–80	772–975	887	5.96	6.54	0.12	0.20			23.7	51.1		25.3	
Yanacocha	7	114	59–65	n/a	777–973	898	6.06	6.48	0.13	0.21			43.0	32.5		24.6	
Young Shiveluch	8	35	56–61	n/a	842–968	914	6.04	6.43	0.11	0.18			40.0	20.0		40.0	
Nisyros	9	212	46–70	n/a	831–1031	957	6.08	6.26	0.13	0.29			80.2	1.9	1.9	15.1	0.9
Oruanui	10	1705	55–77	72–76	686–968	806	6.05	6.86	0.08	0.20			2.6	83.5	0.1	13.8	
Okataina	11–13	1982	51–78	74–78	702–970	813	6.25	6.86	0.06	0.19			2.3	82.7		14.9	
Augustine	14,15	98	54–63	69–76	778–1009	869	5.99	6.66	0.11	0.19			8.2	69.4		22.4	
Crater Lake	16,17	17	51–72	63–74	804–978	926	6.24	6.44	0.2	0.31			41.2	23.5		35.3	
Cardones	19	291	74–76	n/a	851–976	858	6.05	6.67	0.09	0.18		0.3	26.8	51.2		21.6	
Volcanic Systems		**7513**	**46-78**	**63–80**	**686–1031**	**881**	**6.07**	**6.57**	**0.11**	**0.21**		**2.0**	**9.1**	**71.3**	**0.3**	**17.3**	**0.0**
Wooley Creek	20–22	469	51–71	n/a	633–868	774	6.32	6.92	0.01	0.14	1.1			95.7	0.4	2.8	
English Peak	22–24	444	56–71	n/a	616–858	762	6.53	6.97	0.01	0.15	2.7			97.1			0.2
Ashland	22,25	119	51–65	n/a	657–801	761	6.51	7.03	0.01	0.11	1.7		0.8	92.4		5.0	
Tenpeak	22,26,27	928	42–67	n/a	690–975	822	6.14	6.74	0.01	0.09	0.9	1.1		72.7	1.2	22.0	2.2
Tuolumne																	
Kuna Crest	22	204	58–66	n/a	599–807	772	6.74	8.3	0.00	0.13	7.4			92.6			
Transitional KC-eHD	22	322	60–67	n/a	662–814	759	6.66	7.86	0.00	0.11	5.6			94.4			
equigranular Half Dome	22	706	60–69	n/a	646–834	761	6.59	7.93	0.00	0.10	4.2			95.3		0.4	0.1
Transitional eHD-pHD	22	97	62–70	n/a	656–807	764	6.79	7.79	0.00	0.09	1.0			99.0			
porphyritic Half Dome	22	109	65	n/a	659–817	764	6.76	7.83	0.00	0.10	0.9			99.1			
Cathedral Peak	28	101	n/a	n/a	702–816	766	6.38	7.52	0.01	0.09				100.0			
Mt Stuart	22, 27	448	46–71	n/a	655–908	779	6.25	7.03	0	0.12	2.2			92.2		5.4	0.2
Black Peak	22, 27	310	45–69	n/a	532–936	765	6.36	7.09	0	0.13	6.1	0.3	4.2	79.0	0.3	8.4	1.6
Plutonic Systems		**4247**	**42–71**	**n/a**	**532–975**	**775**	**6.39**	**6.98**	**0.01**	**0.12**	**2.8**	**0.3**	**0.3**	**89.1**	**0.3**	**6.5**	**0.7**

* Note that the range of bulk-rock and glass SiO_2 reflects only those analyses for which hornblende and bulk-rock or hornblende and glass pairs are determined.

References: (1) Rooney et al., 2011; (2) Bachmann and Dungan, 2002 (3) Bachmann et al., 2002; (4) Thornber et al., 2008; (5) Pallister et al., 2008; (6) Coombs et al., 2013; (7) Chambefort et al., 2013; (8) Gorbach and Portnyagin, 2011; (9) Klaver et al., 2017; (10) Allan et al., 2017; (11) Deering, 2009; (12) Deering et al., 2011; (13) Shane and Smith, 2013; (14) De Angelis et al., 2013; (15) Larsen et al., 2010; (16) Bacon and Druitt, 1988; (17) Druitt and Bacon, 1989; (18) Nakada et al., 1994; (19) Van Zalinge et al., 2017; (20) Coint et al., 2013a;(21) Coint et al., 2013b; (22) this study; (23) Berry, 2015; (24) Barnes et al., 2017b; (25) Gribble et al., 1990; (26) Chan et al., 2017; (27) Ratschbacher, 2017; (28) Hepeng, 2016

This is a preprint, the final version is subject to change, of the American Mineralogist (MSA)
Cite as Authors (Year) Title. American Mineralogist, in press.
DOI: https://doi.org/10.2138/am-2020-6972

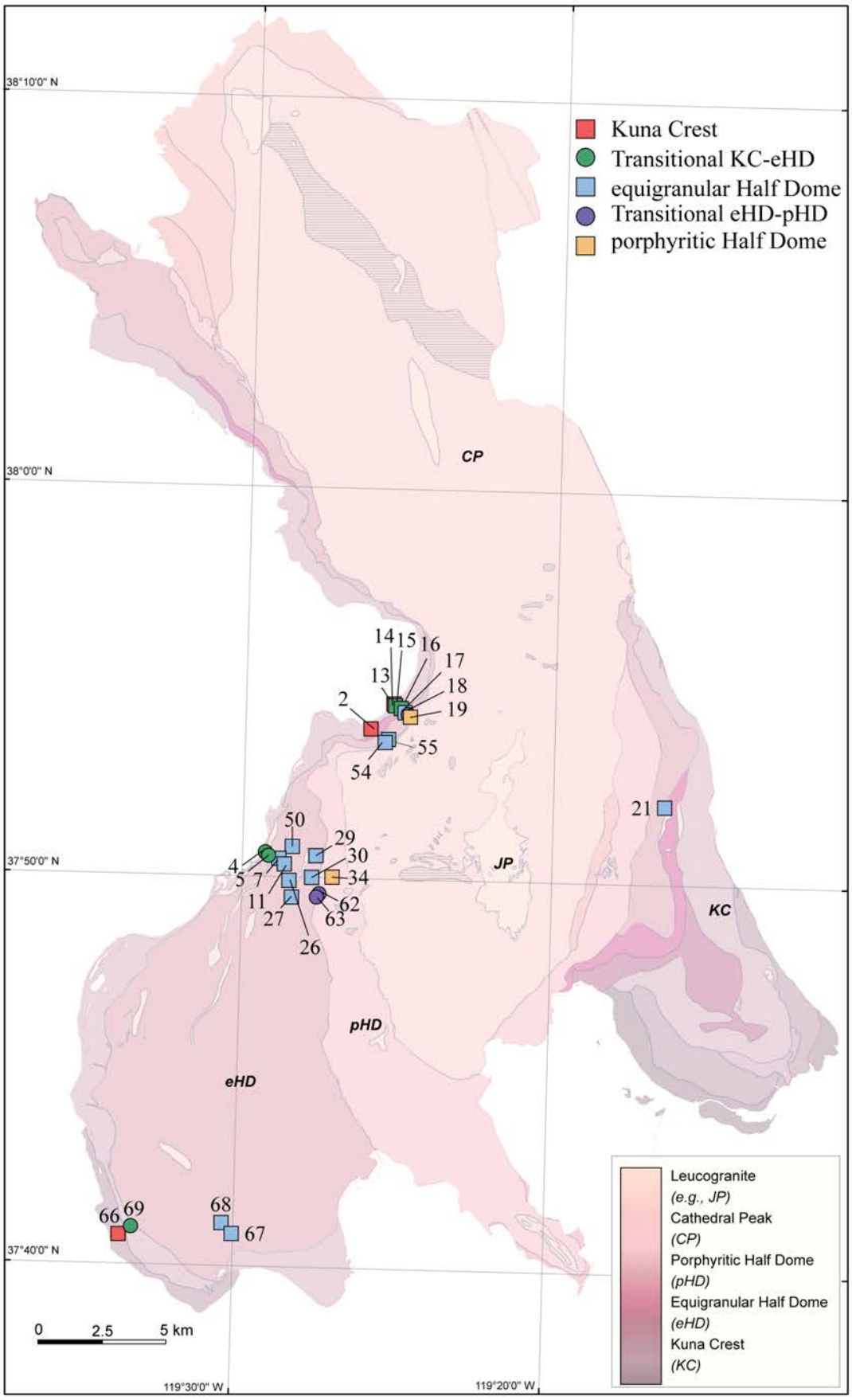

This is a preprint, the final version is subject to change, of the American Mineralogist (MSA)
Cite as Authors (Year) Title. American Mineralogist, in press.
DOI: https://doi.org/10.2138/am-2020-6972

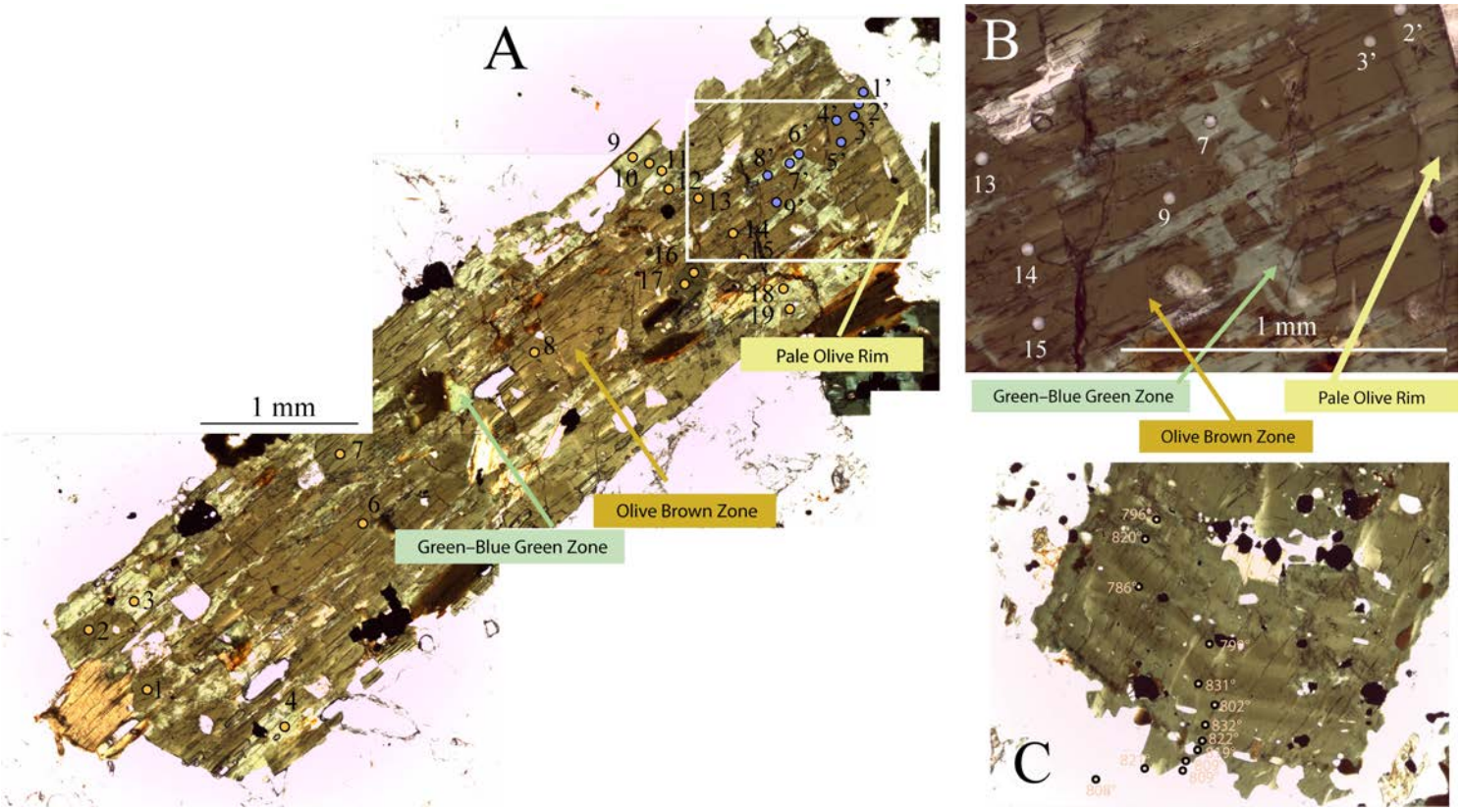

This is a preprint, the final version is subject to change, of the American Mineralogist (MSA)
Cite as Authors (Year) Title. American Mineralogist, in press.
DOI: https://doi.org/10.2138/am-2020-6972

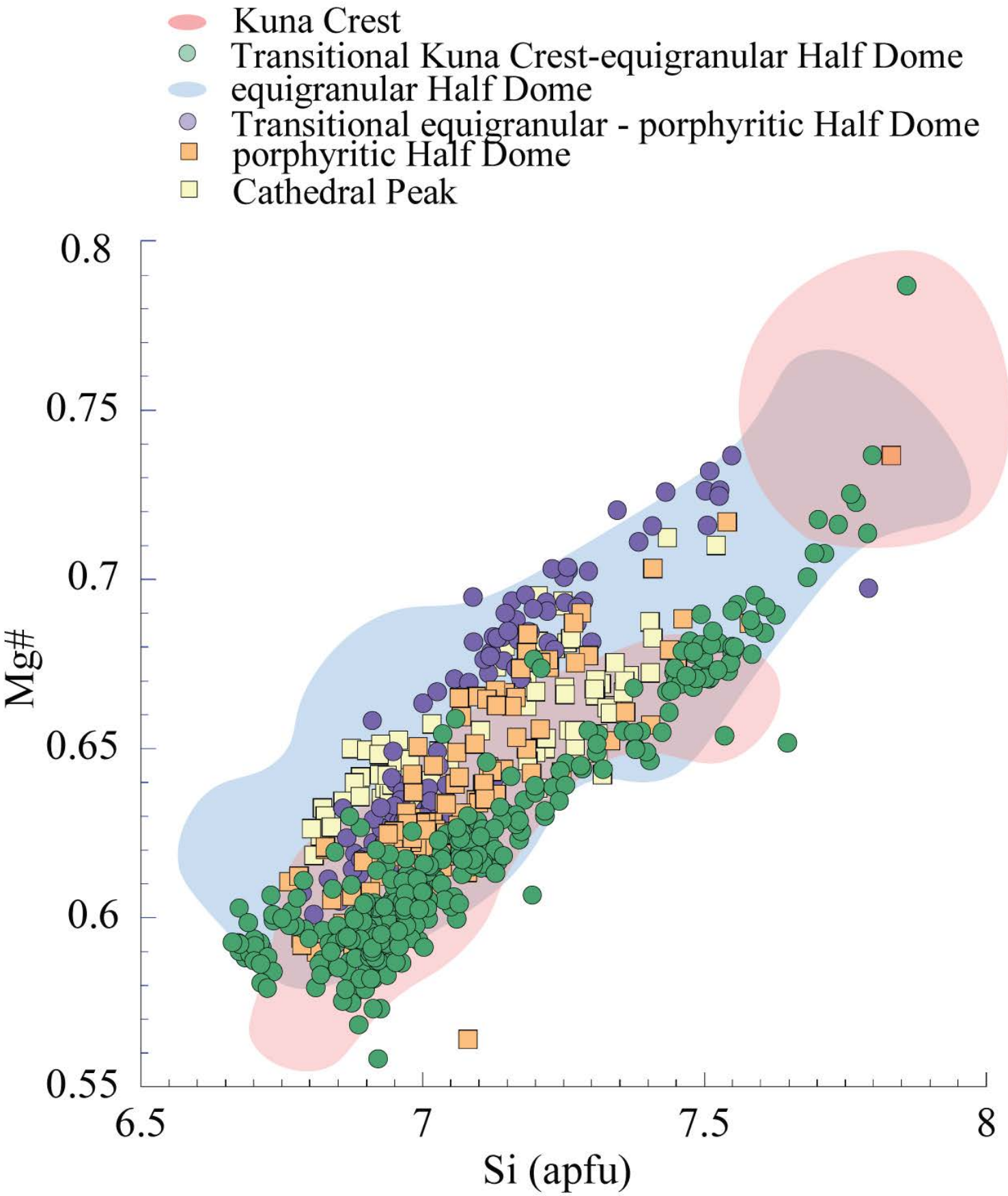

This is a preprint, the final version is subject to change, of the American Mineralogist (MSA)
Cite as Authors (Year) Title. American Mineralogist, in press.
DOI: https://doi.org/10.2138/am-2020-6972

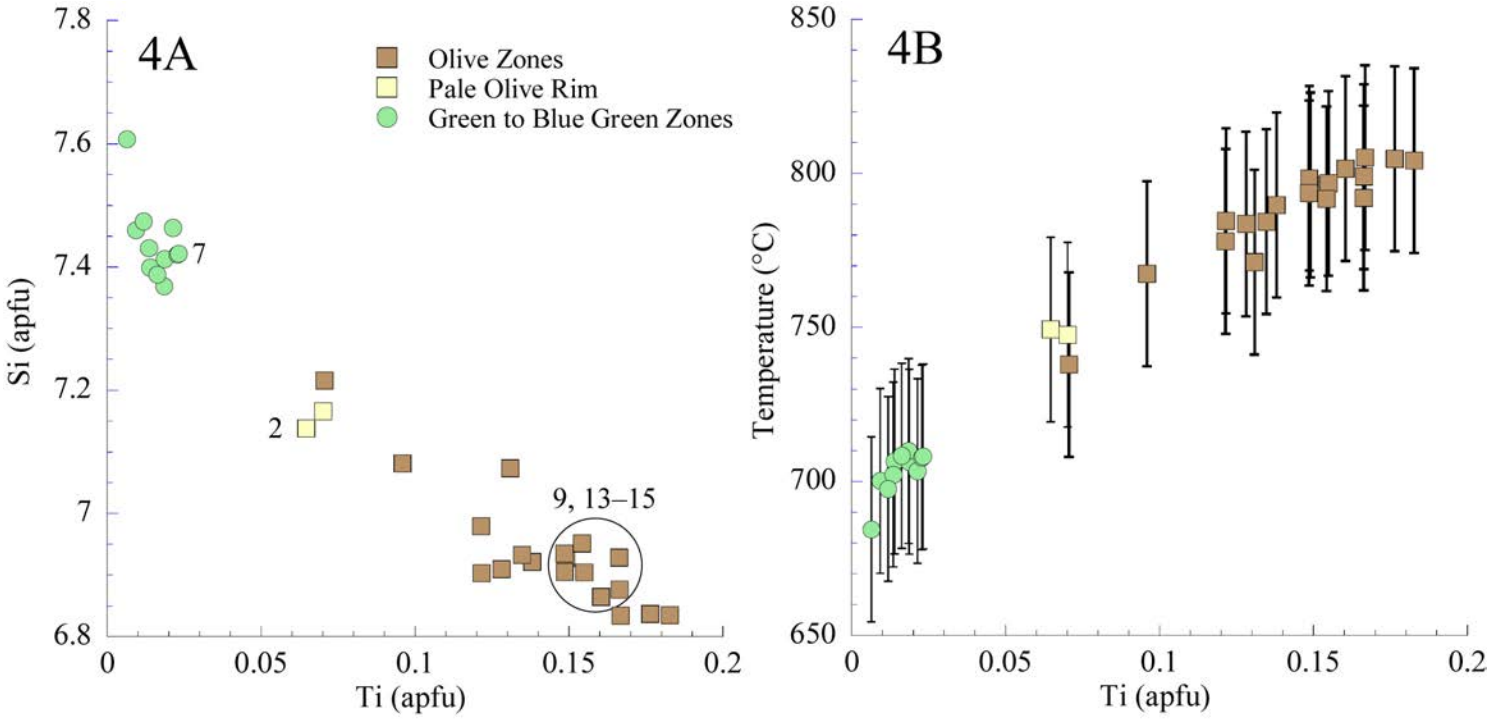

Figure 4

This is a preprint, the final version is subject to change, of the American Mineralogist (MSA)
Cite as Authors (Year) Title. American Mineralogist, in press.
DOI: https://doi.org/10.2138/am-2020-6972

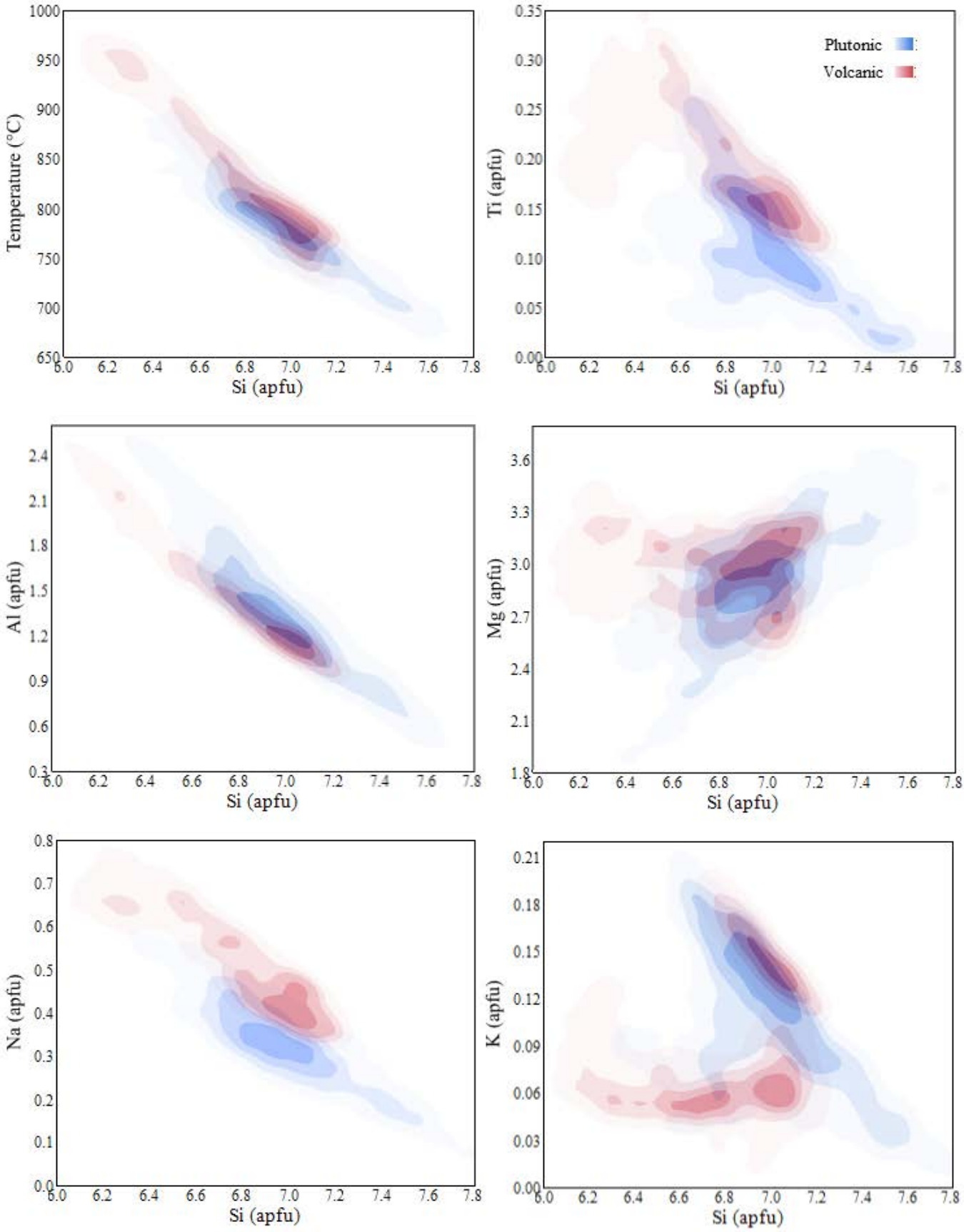

This is a preprint, the final version is subject to change, of the American Mineralogist (MSA)
Cite as Authors (Year) Title. American Mineralogist, in press.
DOI: https://doi.org/10.2138/am-2020-6972

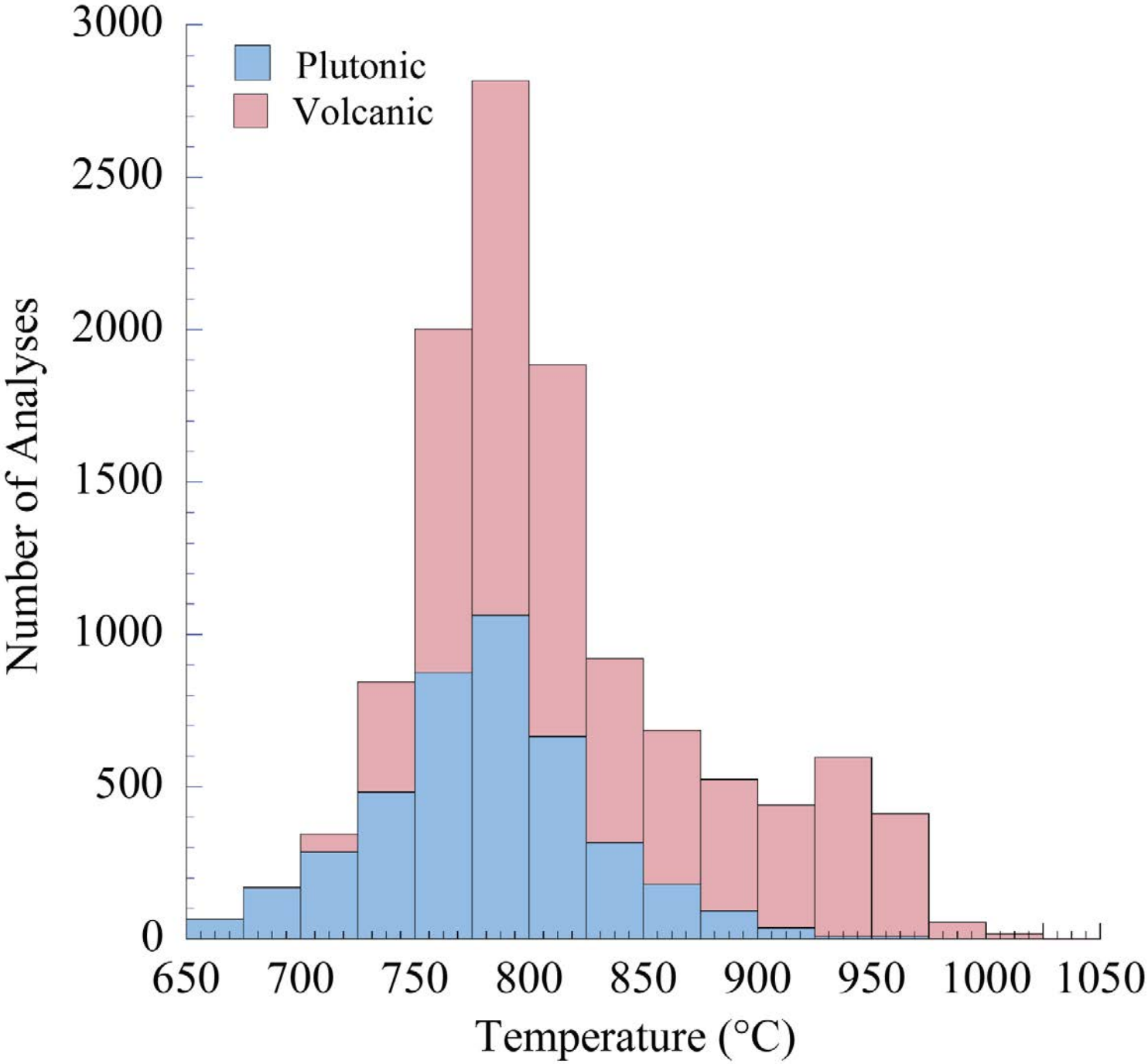

This is a preprint, the final version is subject to change, of the American Mineralogist (MSA)
Cite as Authors (Year) Title. American Mineralogist, in press.
DOI: https://doi.org/10.2138/am-2020-6972

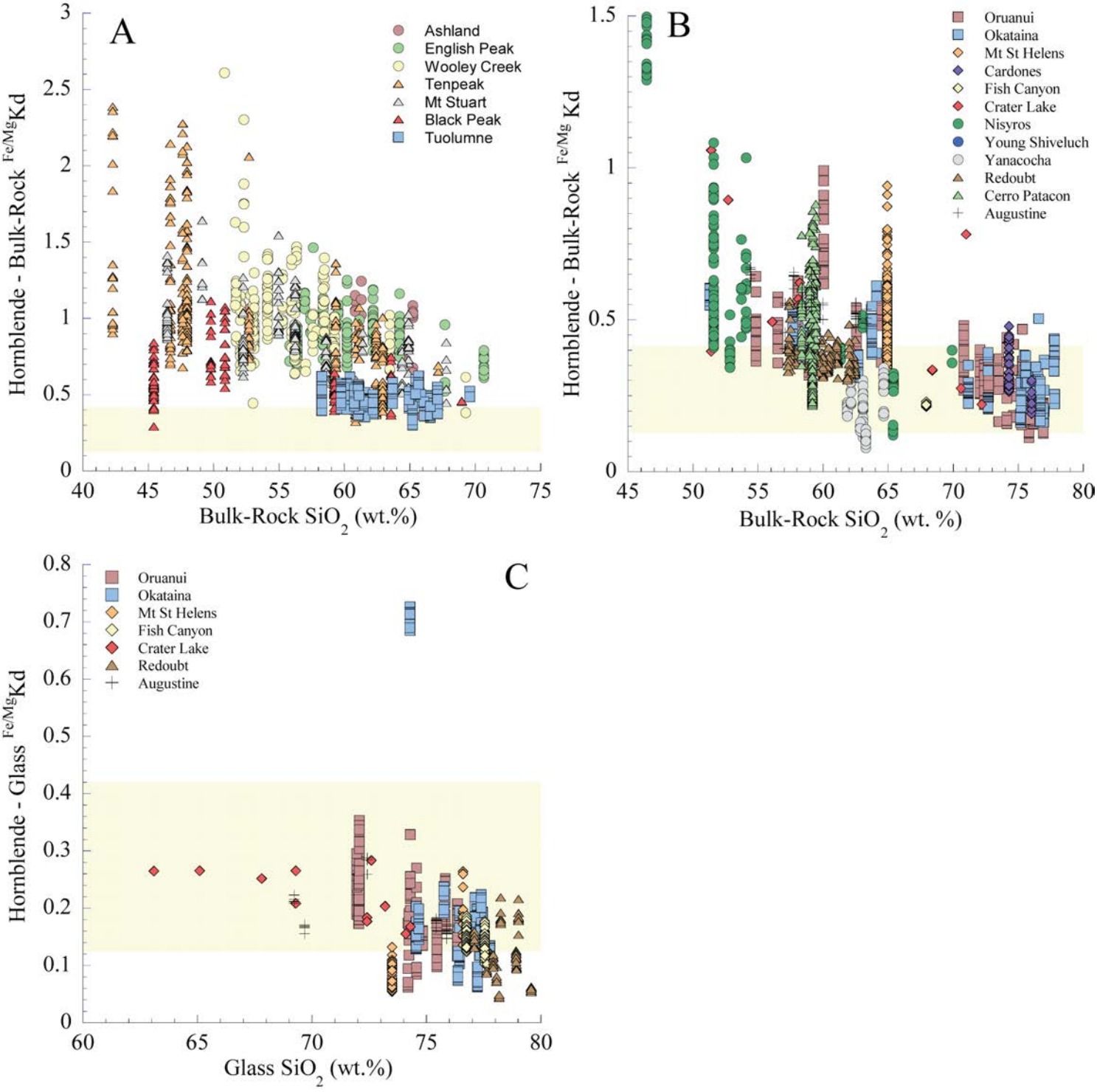

This is a preprint, the final version is subject to change, of the American Mineralogist (MSA)
Cite as Authors (Year) Title. American Mineralogist, in press.
DOI: https://doi.org/10.2138/am-2020-6972

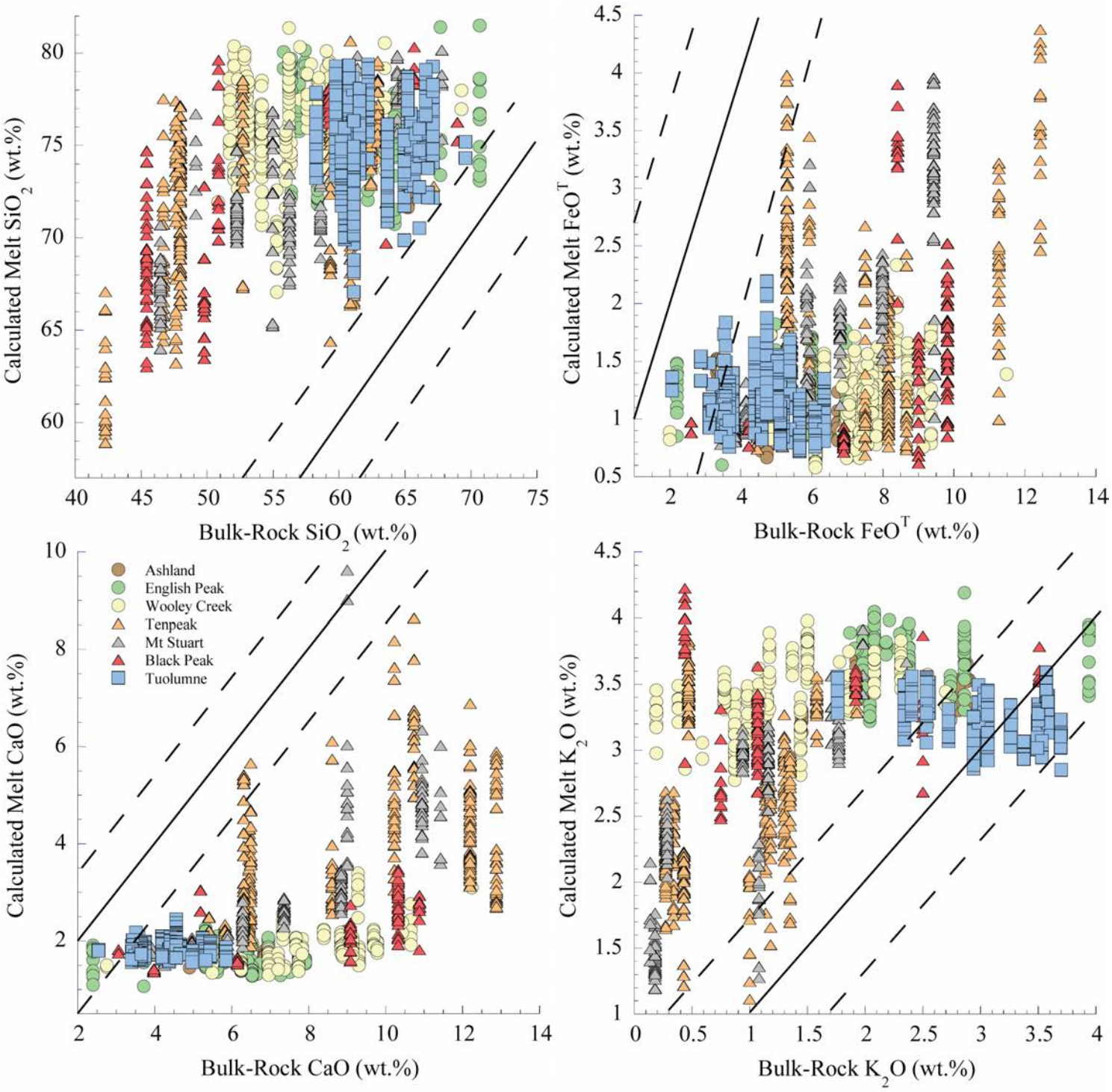

Figure 8

This is a preprint, the final version is subject to change, of the American Mineralogist (MSA)
Cite as Authors (Year) Title. American Mineralogist, in press.
DOI: https://doi.org/10.2138/am-2020-6972

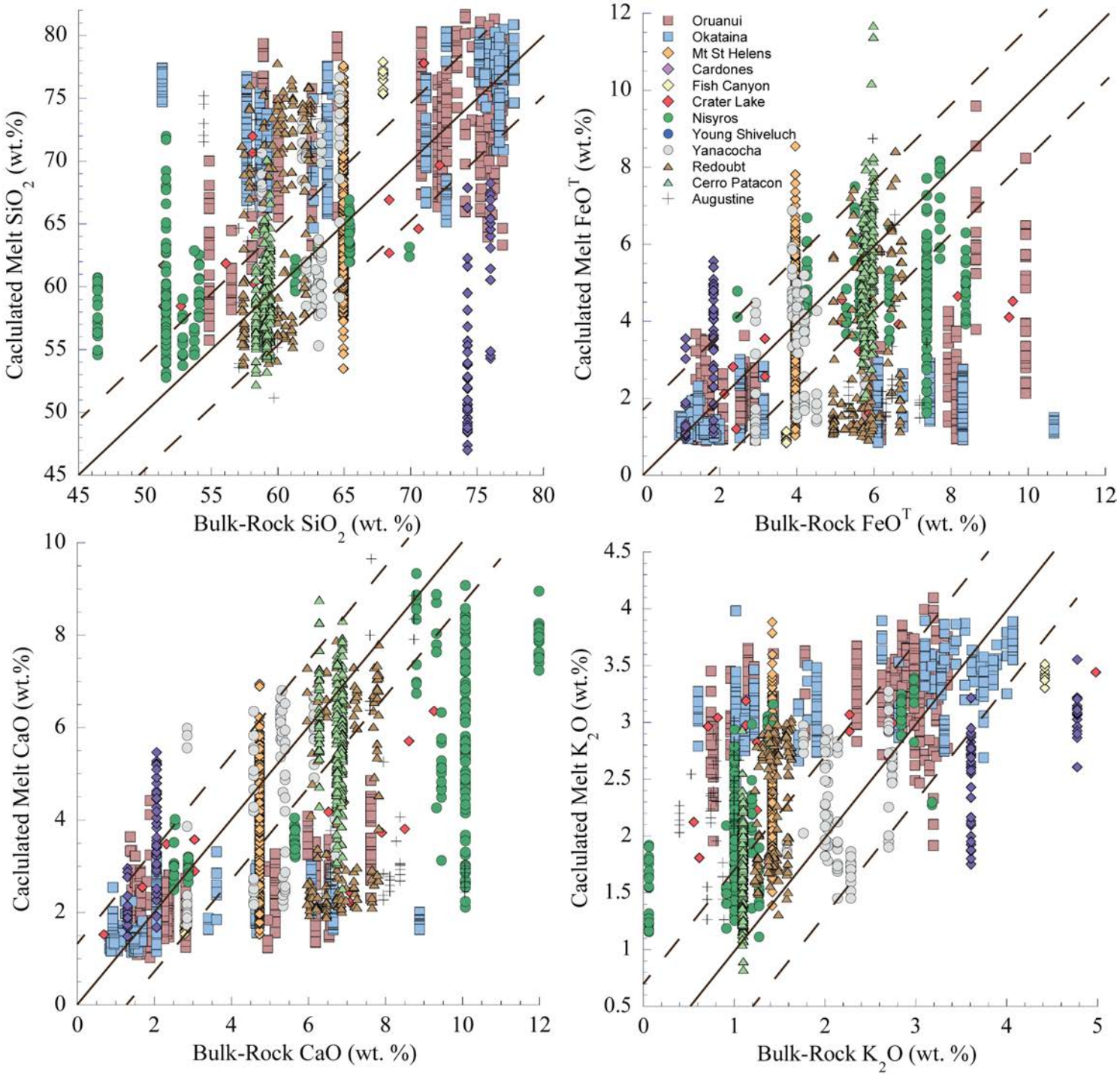

Figure 9

This is a preprint, the final version is subject to change, of the American Mineralogist (MSA)
Cite as Authors (Year) Title. American Mineralogist, in press.
DOI: https://doi.org/10.2138/am-2020-6972

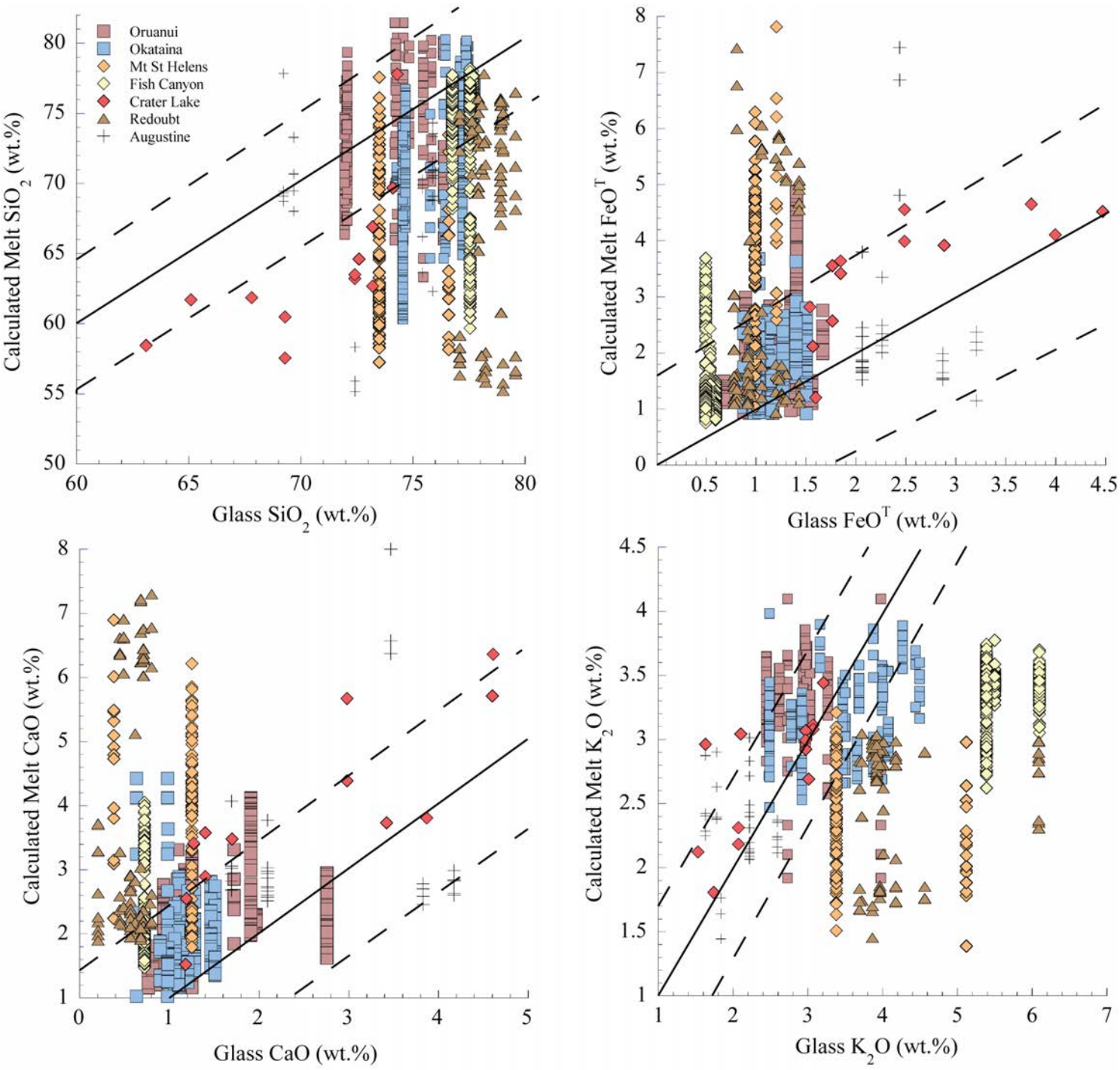

Figure 10